



HAL
open science

Segmental closure of the Mongol-Okhotsk Ocean: insight from detrital geochronology in the East Transbaikalia Basin

Anastasia V Arzhannikova, Elena I Demonterova, Marc Jolivet, Ekaterina A Mikheeva, Alexei V Ivanov, Sergey S Arzhannikov, Valentin B Khubanov, Vadim S Kamenetsky

► To cite this version:

Anastasia V Arzhannikova, Elena I Demonterova, Marc Jolivet, Ekaterina A Mikheeva, Alexei V Ivanov, et al.. Segmental closure of the Mongol-Okhotsk Ocean: insight from detrital geochronology in the East Transbaikalia Basin. *Geoscience Frontiers*, 2022, 13 (1), pp.101254. 10.1016/j.gsf.2021.101254 . insu-03266685

HAL Id: insu-03266685

<https://insu.hal.science/insu-03266685>

Submitted on 22 Jun 2021

HAL is a multi-disciplinary open access archive for the deposit and dissemination of scientific research documents, whether they are published or not. The documents may come from teaching and research institutions in France or abroad, or from public or private research centers.

L'archive ouverte pluridisciplinaire **HAL**, est destinée au dépôt et à la diffusion de documents scientifiques de niveau recherche, publiés ou non, émanant des établissements d'enseignement et de recherche français ou étrangers, des laboratoires publics ou privés.



Distributed under a Creative Commons Attribution - NonCommercial - NoDerivatives 4.0 International License

Journal Pre-proofs

Research Paper

Segmental closure of the Mongol-Okhotsk Ocean: insight from detrital geochronology in the East Transbaikalia Basin

Anastasia V. Arzhannikova, Elena I. Demonterova, Marc Jolivet, Ekaterina A. Mikheeva, Alexei V. Ivanov, Sergey S. Arzhannikov, Valentin B. Khubanov, Vadim S. Kamenetsky

PII: S1674-9871(21)00118-3
DOI: <https://doi.org/10.1016/j.gsf.2021.101254>
Reference: GSF 101254

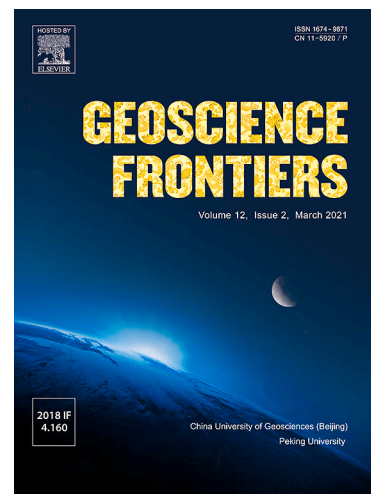
To appear in: *Geoscience Frontiers*

Received Date: 16 February 2021
Revised Date: 30 May 2021
Accepted Date: 17 June 2021

Please cite this article as: A.V. Arzhannikova, E.I. Demonterova, M. Jolivet, E.A. Mikheeva, A.V. Ivanov, S.S. Arzhannikov, V.B. Khubanov, V.S. Kamenetsky, Segmental closure of the Mongol-Okhotsk Ocean: insight from detrital geochronology in the East Transbaikalia Basin, *Geoscience Frontiers* (2021), doi: <https://doi.org/10.1016/j.gsf.2021.101254>

This is a PDF file of an article that has undergone enhancements after acceptance, such as the addition of a cover page and metadata, and formatting for readability, but it is not yet the definitive version of record. This version will undergo additional copyediting, typesetting and review before it is published in its final form, but we are providing this version to give early visibility of the article. Please note that, during the production process, errors may be discovered which could affect the content, and all legal disclaimers that apply to the journal pertain.

© 2021 China University of Geosciences (Beijing) and Peking University. Production and hosting by Elsevier B.V.



Segmental closure of the Mongol-Okhotsk Ocean: insight from detrital geochronology in the East Transbaikalia Basin

Anastasia V. Arzhannikova^{a,*}, Elena I. Demonterova^a, Marc Jolivet^b, Ekaterina A. Mikheeva^a, Alexei V. Ivanov^a, Sergey S. Arzhannikov^a, Valentin B. Khubanov^c, Vadim S. Kamenetsky^{a,c}

^aInstitute of the Earth's Crust, Russian Academy of Sciences, Siberian Branch, Irkutsk, Russia

^bLaboratoire Géosciences Rennes, CNRS-UMR6118, Université de Rennes, Rennes, France

^cGeological Institute, Russian Academy of Sciences, Siberian Branch, Ulan-Ude, Russia

*Corresponding author. Arzhannikova Anastasia, E-mail: arzhan@crust.irk.ru

Abstract

The Late Paleozoic–Early Mesozoic Mongol-Okhotsk Ocean extended between the Siberian and Amur–North China continents. The timing and modalities of the oceanic closure are widely discussed. It is largely accepted that the ocean closed in a scissor-like manner from southwest to northeast (in modern coordinates), though the timing of this process remains uncertain. Recent studies have shown that both western (West Transbaikalia) and eastern (Dzhagda) parts of the ocean closed almost simultaneously at the Early–Middle Jurassic boundary. However, little information on the key central part of the oceanic suture zone is available. We performed U–Pb (LA-ICP-MS) dating of detrital zircon from well-characterized stratigraphic sections of the central part of the Mongol-Okhotsk suture zone. These include the initial marine and final continental sequences of the East Transbaikalia Basin, deposited on the northern Argun-Idemeg terrane basement. We provide new stratigraphic ages for the marine and continental deposits. This revised chronostratigraphy allows assigning an age of ~165–155 Ma, to the collision-related flexure

27 of the northern Argun-Idemeg terrane and the development of a peripheral foreland basin. This
28 collisional process took place 5 to 10 million years later than in the western and eastern parts of the
29 ocean. We demonstrate that the northern Argun-Idemeg terrane was the last block to collide with
30 the Siberian continent, challenging the widely supported scissor-like model of closure of the
31 Mongol-Okhotsk Ocean. Different segments of the ocean closed independently, depending on the
32 initial shape of the paleo continental margins.

33 **Keywords: Detrital zircon U-Pb geochronology; Mongol-Okhotsk collision; East**
34 **Transbaikalian Basin**

35

36 **Handling Editor: R.D. Nance**

37

38 **1. Introduction**

39

40 The closure of the Late Paleozoic–Early Mesozoic Mongol-Okhotsk Ocean is one of the
41 largest and yet highly discussed paleo-geodynamic events in the tectonic evolution of East Asia.
42 As part of the Paleo-Pacific Ocean, the Mongol-Okhotsk Ocean extended between the Siberian
43 and Amur–North China continents (Zonenshain et al., 1990; Sengör and Natal'in, 1996; Yin and
44 Nie, 1996; Zorin, 1999; Parfenov et al., 2003). Relics of this ocean are exposed as meta-sediments
45 and meta-volcanic rocks in the Mongol-Okhotsk Belt that stretches northeastward from the
46 Hangay Mountains of Central Mongolia to the Sea of Okhotsk (Fig. 1). There is still no consensus
47 on many aspects of the evolution of the Mongol-Okhotsk Ocean (see reviews in Kuzmin and
48 Filippova, 1979; Zorin, 1999; Tomurtogoo et al., 2005; Donskaya et al., 2013). Several models
49 have been proposed for the closure of that ocean but the significance of geochronological ages
50 obtained on the subduction/collision related magmatic complexes is still actively discussed. The
51 proposed age of the oceanic closure varies from the Permian to the Early Cretaceous, mainly
52 because of the wide variety and sometimes inaccuracy of the considered data (Nie et al., 1990;

53 Zonenshain et al., 1990; Nie, 1991; Yin and Nie, 1995, 1996; Kuzmin and Kravchinsky, 1996;
54 Davis et al., 1998; Halim et al., 1998; Zorin et al., 1998; Gordienko and Kuzmin, 1999; Zorin,
55 1999; Darby et al., 2001; Kravchinsky et al., 2002; Parfenov et al., 2003; Cogné et al., 2005;
56 Metelkin et al., 2007; 2010; Didenko et al., 2013; Donskaya et al., 2013; Van der Voo et al., 2015;
57 Yang et al., 2015; Demonterova et al., 2017; Jolivet et al., 2017; Arzhannikova et al., 2020; Yi and
58 Meert, 2020 and others). More specifically, the lack of absolute stratigraphic age for the marine
59 and continental deposits and numerous inconsistencies between the paleomagnetic and geological
60 data prevent drawing final conclusions on the timing of the oceanic closure. Most of the
61 geodynamic models imply gradual (scissor-like as coined by Zonenshain et al., 1990) southwest
62 to northeast (in modern coordinates) closure of the ocean and progressive formation of the
63 Mongol-Okhotsk fold belt as suggested by the northeastward decreasing age of the volcano-
64 sedimentary complexes (Zhao et al., 1990; Zonenshain et al., 1990; Scotese, 1991; Kravchinsky
65 et al., 2002; Parfenov et al., 2003; Tomurtogoo et al., 2005; Metelkin et al., 2010). However,
66 recently published U-Pb detrital zircon dates and isotope-geochemical analysis of marine meta-
67 sediments in the eastern Mongol-Okhotsk Belt indicate a westward decrease in the age of the
68 oceanic closure. Along the Dzhagdy transect (Fig. 1) the results revealed no detrital zircon grains
69 younger than 171 Ma in the marine sediments and allowed dating the closure of the eastern
70 Mongol-Okhotsk Ocean to the Early-Middle Jurassic boundary (Sorokin et al., 2020). West of the
71 Dzhagdy transect, around the Upper-Amur Basin (Fig. 1), the width of the Mongol-Okhotsk Belt
72 is very restricted and the closure of the ocean seems to have occurred later than in the Dzhagdy
73 region. Indeed, the stratigraphic age of the sediments and the variations in sediment provenance
74 identified based on U-Pb geochronology of detrital zircon suggest a gradual oceanic closure from
75 the Kimmeridgian–Tithonian to the west to the Berriasian–Valanginian to the northeast of the
76 Upper-Amur Basin (Guo et al., 2017).

77 The Upper Amur Basin is situated in the south-western part of the restricted zone of the
78 Mongol-Okhotsk Belt and belongs to the northern Argun-Idemeg terrane. This terrane forms the

79 northwestern side of the Amur block (Fig. 1) which converged with the Siberian continent during
80 the Late Paleozoic and Mesozoic until complete closure of the Mongol-Okhotsk Ocean
81 (Zonenshain et al., 1990; Parfenov et al., 2003; 2009). A large segment of the most restricted part
82 of the Mongol-Okhotsk Belt to the southwest of the Upper-Amur Basin remains unstudied with
83 respect to determining the absolute age and provenance of the exposed Jurassic sediments. Filling
84 this gap is of major importance: (i) it should help understanding the peculiar geodynamic
85 conditions that lead to such a restricted belt along that segment of the Mongol-Okhotsk collision
86 zone and (ii) it will confirm or infirm that this part of the belt is younger than the Dzhagdy segment,
87 testing the validity of the widely supported hypothesis of a scissor-like northeastward oceanic
88 closure. In this work we present the results of U-Pb (LA-ICP-MS) dating of detrital zircons from
89 both marine terrigenous and continental deposits of the East Transbaikalia Basin on the northern
90 Argun-Idemeg terrane (Fig. 1). We provide new stratigraphic framework for the sediments,
91 identify the source areas, and date the transition from marine to continental depositional
92 environment. Finally, we discuss the timing of complete closure of the Mongol-Okhotsk Ocean in
93 this region and place it within the context of the general evolution of the Mongol-Okhotsk orogeny.

94

95 **2. Geological setting**

96 **2.1. Geology of the Argun-Idemeg terrane and East Transbaikalia Basin**

97

98 The Argun-Idemeg terrane is located southeast of the Mongol-Okhotsk suture zone (Fig.
99 1). According to Zonenshain et al. (1990), Parfenov et al. (2010), Wu et al. (2011) and Sun et al.
100 (2013), it has a Neoproterozoic granite-metamorphic basement overlain by sedimentary series
101 showing several unconformities related to tectonic and magmatic events. Recently published U-
102 Pb ages of magmatic zircons from granodiorites and gneisses in the Erguna block (northeastern
103 part of the Argun-Idemeg terrane) revealed the Paleoproterozoic age of the basement (Sun et al.,
104 2019; Liu et al., 2020). Several marine transgressions, resulting in the accumulation of sandstones,

105 clay, and carbonates took place on the Erguna block in the Late Proterozoic–Early Cambrian, from
106 the Silurian to the Early Carboniferous and in the Early–Middle Jurassic. Interruptions in
107 sedimentation are associated with periods of tectonic deformation, erosion, and volcanic activity
108 in the Late Cambrian–Ordovician, at the Middle to Late Paleozoic transition and from the Early
109 Permian to the Early Triassic (Starchenko, 2010). U-Pb dating of magmatic zircons from
110 granitoids of the Erguna block allowed constraining the spatial and temporal distribution of
111 granitic magmatism in the area (Wu et al., 2011) (Fig. 2). According to this data, most of intrusions
112 were emplaced during the Early Paleozoic (416–517 Ma), Late Triassic–Early Jurassic (182–220
113 Ma) and Early Cretaceous (118–132 Ma). Two minor stages of granitic magmatism occurred in
114 the Neoproterozoic (792–927 Ma) and Late Paleozoic–Early Mesozoic (244–336 Ma).

115 The last marine stage is associated with the formation of the Mesozoic East Transbaikalia
116 Basin (Fig. 3, see location on Fig. 1) along the Mongol-Okhotsk Ocean subduction zone. As
117 indicated by the occurrence of marine fauna assemblages, marine sedimentation lasted from the
118 Pliensbachian to the Aalenian (Starchenko, 2010). During that period, thick accumulations of
119 marine clastic sediments were deposited, divided into the proximal coastal environments of the
120 Algachi-Kalgan zone and the more distal environments of the Onon-Gazimur zone (Fig. 4). Four
121 depositional stages have been individualized: 1 – initial flexure in the Onon-Gazimur zone with
122 accumulation of psammitic-pelitic deposits of the Ikagiisk Fm., 2 – enhanced subsidence and basin
123 widening with fully marine sedimentation in the Onon-Gazimur zone (Tamenginsky Fm.) and
124 onset of coastal marine sedimentation in the Algachi-Kalagan zone (Akatui Fm.), 3 – marine
125 regression and deposition of the Sivachinsky and Bazanov molasse fms., 4 – a final stage showing
126 an initial deepening (Gosudarevsky Fm.) followed by regression (Kavykuchinsky Fm.) in the
127 Onon-Gazimur marine basin and discontinuous proximal sedimentation in the Algachi-Kalgan
128 zone (Bokhtin Fm.). A hiatus in sedimentation is possibly associated with the transition between
129 the transgression and regression phases in the Onon-Gazimur zone. Based on the large amount of
130 plant macro-fossils preserved in the sediment, complete regression occurred during the Bajocian

131 as marine terrigenous sedimentation was replaced by continental coarse-grained molasse deposits
132 of the Upper Gazimur Fm. (Starchenko, 2010).

133 Based on this stratigraphy, the closure of the Mongol-Okhotsk Ocean in the East
134 Transbaikalia area is dated to the early Middle Jurassic at the transition from marine to continental
135 sedimentation (Zorin, 1999; Parfenov et al., 2003). The series are dated from paleontological and
136 paleofloristic data (Starchenko, 2010), as no absolute age exists. However, a younger age for the
137 oceanic closure can be inferred from the Late Jurassic change in geochemical composition of the
138 East Transbaikalia volcanic rocks from shoshonite-latite, typical of active continental margins, to
139 trachybasalt, typical of intracontinental volcanism (Khlif et al., 2017). ^{40}Ar - ^{39}Ar dating of
140 shoshonite-latites of the Akatui intrusive massif within the East Transbaikalia Basin (Fig. 3A)
141 indicates emplacement ages from 162 Ma to 155 Ma (Sasim et al., 2016).

142

143 **2.2. Stratigraphy of the East Transbaikalia Basin.**

144 **2.2.1. The proximal Algachi-Kalagan zone.**

145

146 The Akatui Fm. represents the onset of Jurassic coastal-marine deposits and is assigned to
147 the Late Pliensbachian (J_1) (Starchenko, 2010). The basal deposits are composed of conglomerates
148 and breccias resting unconformably on the Devonian basement. The series evolves upward to
149 sandstones, siltstones, and argillites.

150 The Bazanov Fm. conformably overlies the Akatui Fm., sometimes with gradual transition
151 and evidence of intra-formation erosion phases. The deposits are largely composed of polymictic
152 pebbly conglomerates interlayered with gravel conglomerates and sandstones. Some few siltstone
153 interlayers are also observed. Sandstones are mainly confined to the central part of the formation,
154 while the upper and lower levels consist mainly of conglomerates. The Bazanov Fm. is poorly
155 characterized in terms of paleontology. The age of the formation (Late Pliensbachian–Early

156 Toarcian (J_1) is assigned based on the correlation with the Sivachinsky Fm. of the distal Onon-
157 Gazimur zone.

158 Most of the Bokhtin Fm., uppermost among the coastal-marine formations, conformably
159 overlies the Bazanov Fm. and corresponds in age to the Toarcian–Early Aalenian (J_{1-2}) based on
160 faunal remains. The formation is composed of poorly-sorted polymictic and arkosic sandstones,
161 gritstones, siltstones, clay, and pebble conglomerates. The whole series corresponds to turbidite
162 deposits of the inner shelf and coastal plains.

163 The Upper Gazimur Fm. that covers both the proximal and distal zone is composed of
164 lacustrine and alluvial coarse-grained deposits and overlies the Jurassic marine deposits
165 conformably or unconformably depending on the location. The deposits are represented by
166 conglomerates with boulder-size clasts rarely interlayered with sandstones in the lower and upper
167 parts of the section and sandstones and gritstones in its central part. Plant remnants are found
168 throughout the deposits but are not allowing dating. According to its position above the Toarcian-
169 Early Aalenian Bazanov Fm., and above the Early Bajocian Kavykuchinsky Fm. in the distal
170 Onon-Gazimur zone (see below in section 2.2.2), the Upper Gazimur Fm. is roughly dated to the
171 Late Bajocian–Early Bathonian (J_2). This sedimentary formation indicates the change of the
172 marine to continental sedimentation mode.

173

174 **2.2.2. The distal Onon-Gazimur zone.**

175

176 In the distal depositional zone, the Ikagiisk Fm. represents the onset of Jurassic marine
177 sedimentation. The basal deposits rest unconformably on the Carboniferous basement and are
178 composed of conglomerates, gritstones and thin layers of breccia. The rest of the formation
179 consists of argillites and siltstones, the lower part being sandier and the upper part more clay-rich.
180 Based on numerous marine mollusk fossils, the formation is dated to the Pliensbachian.

181 The Tamenginsky Fm. conformably overlies the Ikaginsk Fm. The base of the
182 Tamenginsky Fm. is composed of a relatively thin layer of breccias and conglomerates. The rest
183 of the deposits consist of interbedded siltstones, argillites and sandstones, with rare interlayers and
184 lenses of gritstones and conglomerates. Again, based on marine mollusk fossils, the formation is
185 dated to the Late Pliensbachian.

186 The Sivachinsky Fm. is composed of polymictic small-to-large pebble conglomerates
187 interlayered with sandstones, siltstone, and unsorted micro-conglomerates. It conformably
188 overlaps the Tamenginsky Fm., usually through a gradual facies transition. Like the Bazanov Fm.
189 in the proximal area, the Sivachinsky Fm. has a threefold structure in many sections – the tops and
190 bottoms are mainly represented by conglomerates, and the middle part – by sandstones. The age
191 of the formation (end of Pliensbachian–beginning of Toarcian) was determined from the
192 ammonoid *Amaltheus viligaensis* and clam *Ochotochlamys grandis* found at the base as well as
193 from the Early Toarcian ammonoids *Tiltoniceras* sp. indet. and *Kedonoceras* sp. indet. at the top
194 (Starchenko, 2010).

195 The Gosudarevsky Fm. in some places overlays the Sivachinsky Fm., while in places it
196 rests directly on the pre-Jurassic basement. In its lower part the formation is represented by
197 interbedded polymictic sandstones, siltstones and argillites, while the upper part is composed of
198 siltstones and argillites with very rare thin interlayers of calcareous sandstones and horizons of
199 small-grained pebble conglomerates. The frequency of conglomerate interlayers and the size of
200 the pebbles increase toward the top of the formation. Based on ammonoids and mollusks fossils,
201 a Toarcian age has been established for that formation.

202 Being the last marine deposits in the Onon-Gazimur zone, the Kavykuchinsky Fm.
203 overlaps the Gosudarevsky Fm. with a gradual transition. The lower parts of the formation are
204 composed of sandstones, gritstones and conglomerates with interlayers of siltstones. The relatively
205 coarser upper part of the formation is composed of medium- to large-pebble conglomerates and
206 coarse-grained sandstones. Based on the occurrence of bivalve mollusks *Aguilerella khudyavi* in

207 the lower part of the formation and *Mytiloceras* ex gr. *Polyplocus* and *Mytiloceras* ex gr.
208 Lucifer in the upper part, an Early Aalenian to the Early Bajocian age has been ascribed to the
209 Gosudarevsky Fm. (Starchenko, 2010).

210

211 **3. U-Pb (LA-ICP-MS) dating of detrital and magmatic zircons**

212

213 Detrital zircon grains were extracted from samples of the marine Akatui, Bazanov, Bokhtin
214 and Sivachinsky fms. as well as from the continental Upper Gazimur Fm. (Fig. 4). Magmatic
215 zircons from dikes cutting through the sediment deposits of the Bokhtin and Upper Gazimur fms.
216 were also dated using the same method. U-Pb dating of those grains will provide absolute age
217 constrains for the sedimentary deposits of the East Transbaikalia Basin and allow tracing the
218 evolution of the sediment source areas. Indeed, U-Pb dating of detrital zircon allows determining
219 the lower age limit for sedimentary deposits and dating of zircon from cutting dikes provides the
220 information on the upper age limit for sediments.

221

222 **3.1. Methods**

223

224 Zircon grains were separated using the conventional method before a final hand picking of
225 crystals under a binocular microscope. Over 100 zircon grains were collected from each sediment
226 samples. U-Pb analysis was done at the Geological Institute, Russian Academy of Sciences,
227 Siberian Branch (Ulan-Ude, Russia) by laser ablation inductively coupled plasma mass
228 spectrometry using a high-resolution mass spectrometer Element XR (Thermo Fisher Scientific)
229 coupled to an UP-213 laser (New Wave Research). The instrumental settings and the analytical
230 procedure can be found in Khubanov et al. (2016) and Buyantuev et al. (2017). The ages were
231 calculated relative to the primary zircon standard 91500 (Wiedenbeck et al., 1995) and the quality
232 of the analyses was monitored through analyses of secondary Plešovice (Sláma et al., 2008) and

233 GJ-1 (Jackson et al., 2004) zircon standards. Relative uncertainties for Plesovice and GJ-1 zircon
234 standards were: 1%–2.3% for $^{208}\text{Pb}/^{232}\text{Th}$, 2.1%–2.6% for $^{207}\text{Pb}/^{206}\text{Pb}$, 1.1%–2.6% for $^{206}\text{Pb}/^{238}\text{U}$
235 and 2%–2.5% for $^{207}\text{Pb}/^{235}\text{U}$ leading to the calculated age values within 2% of the recommended
236 age values. All data were processed using the GLITTER program (Griffin et al., 2008). For plotting
237 kernel density estimates only ages with less than 10% of discordance were used. Kernel density
238 estimates and Concordia diagrams were plotted using the IsoplotR software (Vermeesch, 2012;
239 2018).

240 Zircon separated from acidic dike samples were dated by the same technique at the
241 University of Tasmania (Hobart, Australia). The instrument was an Agilent 7500cs quadrupole
242 ICP-MS with a 193 nm Coherent Ar-F gas laser and the Resonetics S155 ablation cell. The width
243 of the laser beam was 25 μm . The primary standard for age calculation was again the zircon
244 standard 91500 (Wiedenbeck et al., 1995) and the secondary standard was Temora (Black et al.,
245 2003).

246

247 **3.2. Results**

248

249 The Akatui Fm. was sampled from an exposure in the interfluvium between the Ozoran and
250 Mankechur Rivers (sample Ln-15-24, 50°44.798'E, 117°50.250'E, alt. 950 m) (Fig. 5A). The
251 formation is represented by fine-grained sandstones intercalated with siltstones. Concordant ages
252 were obtained for 51 individual zircon grains (Supplementary Data, Table S1). These ages are
253 distributed into two populations: 162–179 Ma (15% of grains) and 232–268 Ma (65% of grains).
254 Some outliers with ages of 289, 301, 326, 445, 473, 480, 592, 897 and 937 Ma are also present.
255 These outliers do not represent statistically reliable populations (3% or more) and are not
256 considered for discussion. The youngest zircon in the sample has an age of 162.3 ± 4.4 Ma (Fig.
257 6A).

258 The Bazanov Fm. was sampled from a sandy interlayer in the conglomerate member
259 exposed near the settlement of Mankechur (sample Ln-15-16, 50°43.752'N, 117°52.112'E, alt.
260 832 m) (Fig. 5B). The conglomerates are polymictic, with the pebble composition dominated by
261 granites, syenites, and sediments. A total of 94 concordant individual zircon ages were obtained
262 (Supplementary Data, Table S2). The age distribution is similar to that of sample Ln-15-24 with
263 two main populations: 158–192 Ma (35% of grains) and 232–269 Ma (38% of grains). However,
264 a secondary population at 424–491 Ma (9%) is also present together with a few outliers. The
265 youngest zircon has an age of 158.4 ± 4.0 Ma (Fig. 6B).

266 The Bokhtin Fm. was sampled in a section along the left bank of the Malaya Borzya River
267 (sample Ln-15-43, 50°44.783'N, 118°6.669'E, alt. 739 m). The formation therein is composed of
268 interlayered siltstones, sandstones, gritstones and conglomerates intruded by two acidic dikes (Fig.
269 5C). One of these dikes (sample Ln-15-40), yielded a U-Pb age of 131.76 ± 0.71 Ma
270 (Supplementary Data, Table S3). The sediment sample was taken from a sandstone interlayer
271 where 110 concordant individual zircon ages (Supplementary Data, Table S4) were obtained. The
272 age distribution shows a unique well-defined peak at 239–268 Ma (93% of grains), and few outliers
273 with ages up to 1066 Ma. The youngest zircon has an age of 166.2 ± 5.0 Ma (Fig. 6C).

274 The Sivachinsky Fm. was sampled in a small exposure near the settlement of Kirillikha
275 (sample Ln-15-47, 50°55.700'N, 117°28.704'E, alt. 892 m). The series is represented by
276 conglomerates interlayered with sandstones. The sample was taken from a sandstone interlayer
277 (Fig. 5D). Among 51 concordant individual zircon ages (Supplementary Data, Table S5) three
278 young zircon grains with ages of 165, 189 and 190 Ma were found. A major age population at
279 237–295 Ma (69% of grains) is associated with a secondary population at 480–499 Ma (10% of
280 grains) and few outliers. The youngest zircon in the sample from the Sivachinsky Fm. has an age
281 of 165.0 ± 4.5 Ma (Fig. 6D).

282 The continental Upper Gazimur Fm. was sampled from a section on the right bank of the
283 Borzya River opposite the settlement of Akurai (sample Ln-15-9, 50°47.433'N, 117°07.210'E, alt.

284 767 m). The sediment is composed of poorly sorted pebble conglomerates interlayered with
285 sandstones wherefrom the sample for detrital zircon dating was taken (Fig. 5E). A total of 96
286 concordant individual zircon ages were obtained (Supplementary Data, Table S6). The zircon age
287 distribution differs from that in the marine formation samples. Besides a well-defined population
288 at 231–268 Ma (30% of grains), a second major population of ages is spread between 280 Ma and
289 512 Ma (52% of grains), with a predominance of Devonian (16%) and Early Paleozoic (15%) ages.
290 Several minor populations are also present with Jurassic: 155–162 Ma (3% of grains, the youngest
291 155.2 ± 4.0 Ma), and Paleoproterozoic: 1697–1715 Ma (3% of grains) and 1787–1810 Ma (3% of
292 grains) ages. Finally, a few Neo- and Mesoproterozoic single grains are spread between the
293 Paleozoic and Paleoproterozoic populations (Fig. 6E).

294 A syenite dike intruded through the Upper Gazimur Fm. deposits was sampled near the
295 settlement of Shonoktui (sample Ln-15-48, $50^{\circ}46.269'N$, $117^{\circ}17.048'E$, alt. 846 m) and dated at
296 127.33 ± 0.51 Ma (zircon U-Pb) (Fig. 7B, Supplementary Data, Table S3).

297

298 4. Discussion

299 4.1. Depositional age of the sedimentary formations

300

301 The detrital geochronology results presented above can be used to discuss the stratigraphy and
302 to better estimate the age of the Jurassic sedimentary formations in the East Transbaikalia Basin. They
303 also allow discussing the timing of transition between marine and continental depositional
304 environments in the basin (Fig. 8). According to the age of the youngest zircon in the sample, the
305 coastal-marine Bazanov Fm. is younger than 158.4 ± 4.0 Ma. Since the Bokhtin Fm. overlies the
306 Bazanov one, it can be concluded that both formations are younger than ~ 158 Ma. Similarly, the
307 underlying Akatui Fm. is not older than 162.3 ± 4.4 Ma, in accordance with the age of the youngest
308 zircon analyzed in sample Ln 15-24. The Akatui Fm. is affected by the Akatui intrusive complex that
309 provided ^{40}Ar - ^{39}Ar ages on amphiboles ranging from 162 Ma to 155 Ma (Sasim et al. 2016). Given

310 the maximum age of the overlying Bazanov Fm., we suggest that the Akatui Fm. was deposited
311 between 162 Ma and 158 Ma, synchronous to the magmatic activity. The Sivachinsky Fm. is considered
312 as a distant equivalent of the Bazanov Fm. (Starchenko, 2010), but the age of the youngest detrital
313 zircon in the Sivachinsky Fm. provides an older estimate of the maximum age of the formation at
314 165.0 ± 4.5 Ma. Again, based on detrital geochronology, the maximum age of the continental Upper
315 Gazimur Fm. is 155.2 ± 4.0 Ma. The data obtained from the dikes (131.76 ± 0.71 Ma and $127.33 \pm$
316 0.51 Ma, Fig. 7) intruding into the Bokhtin and Upper Gazimur fms., respectively, provide a very
317 wide range for the minimum age of these upper formations. Considering the widespread
318 occurrence of the Late Jurassic–Early Cretaceous magmatism (ages are distributed between 164
319 Ma and 118 Ma) in the region, including acidic magmatism with a large number of zircons
320 (Zakharov, 1972; Troshin, 1978; Tauson et al., 1984; Ivanov et al., 2015; Sasim et al., 2016), it
321 should be assumed that zircon grains of these ages found in the sediments are reflecting syn-
322 sedimentary volcanism. Thus, in this particular case the ages of the youngest zircons in the
323 sediments can be also considered as the true depositional age (Dickinson and Gehrels, 2009;
324 Rossignol et al., 2019).

325 To summarize, we propose that the studied marine series were deposited during the late
326 Middle Jurassic rather than the Early Jurassic, as previously assumed (Starchenko, 2010). The
327 change from marine to continental depositional environments occurred in the Oxfordian–
328 Kimmeridgian (formally, between overlapping ages of 158.1 ± 4.0 Ma and 155.2 ± 4.0 Ma).

329

330 **4.2. Provenance of detrital zircons and time of the final marine regression in Eastern** 331 **Transbaikalia**

332

333 The major detrital zircon age populations described above from the sediments fit with local
334 source areas. The youngest age population of 155–192 Ma is present in all the formations but the
335 Bokhtin Fm. where only a single grain of this age was recovered. This population is generally

336 minor, except in the Bazanov Fm. where it represents a major peak. The youngest zircons of this
337 population (155–174 Ma) correspond in age to the Middle-Late Jurassic magmatism widespread
338 in the region and widely intruding the Jurassic marine sedimentary deposits (Starchenko, 2010).
339 As for the Early Jurassic zircon grains, magmatism of this age is absent within the East
340 Transbaikalia Basin (Starchenko, 2010). However, extensive zircon U-Pb dating of volcanic rocks
341 in the Chinese part of the Erguna block revealed Early Jurassic ages of 179–200 Ma (Wu et al.,
342 2011; Sun et al., 2013 and references therein). It is thus probable that Early Jurassic magmatism
343 also took place within the Russian part of the Erguna block, but that the small number of available
344 geochronological data did not yet allow its discovery. Therefore, we suggest that the Early Jurassic
345 zircon grains found in the Akatui and Bazanov formations are also derived from a local source.

346 The main zircon age population observed within all marine formations and the second
347 largest in the continental formation falls within the range of 231–295 Ma, which corresponds to
348 the Permian-Triassic granitoid magmatism widespread within the Erguna block (Wu et al., 2011;
349 Sun et al., 2013) (Figs. 2, 3). Zircons with ages from 280 Ma to 500 Ma are represented by a very
350 limited number of grains in all marine formations. However, in the continental Upper Gazimur
351 Fm., they represent more than half of the dated grains with a predominance of Devonian and Early
352 Paleozoic ages. The Early Paleozoic granitoids have a large distribution within the Erguna block
353 (Wu et al., 2011), and are also widely spread throughout the Siberian continent including the
354 Olekma granite complex adjacent to the Mongol-Okhotsk suture to the north (Starchenko, 2010)
355 (Figs. 2, 3). Late Devonian sedimentary-volcanic complexes and rhyolites occur within the Onon
356 block which, being an island-arc, forms one segment of the Mongol-Okhotsk Belt west of the
357 Erguna block (Zorin, 1999), but are almost completely absent from the Erguna block (Starchenko,
358 2010; Wu et al., 2011; Sun et al., 2013; Sun et al., 2019) (Figs. 2, 3). This observation suggests a
359 source area to the west for the Upper Gazimur continental deposits.

360 Single zircon grains ranging in age from 500 Ma to 900 Ma distributed in all the formations
361 correspond in age to the Neoproterozoic granites of the Erguna block, again suggesting a local

362 sediment source (Wu et al., 2011; Sun et al., 2013; Smirnova and Sorokin, 2019; Goraienko et al.,
363 2019) (Fig. 3). The oldest zircon grains (1.6 Ga to 1.8 Ga) were found in the continental deposits
364 of the Upper Gazimur Fm. (6% of grains) (Fig. 6E). Paleoproterozoic rocks are only found in the
365 northeastern part of the Erguna block (two samples with ages of 1785 Ma and 1860 Ma (Sun et
366 al., 2019)), far from the study area, but widespread throughout the Siberian continent (Figs. 2, 3).
367 Granitoids with an age of 1.5–2 Ga are found within the Selenga-Stanovoy orogenic belt (Karsakov
368 et al., 2005), located immediately to the north of the Mongol-Okhotsk suture in the study area (Fig.
369 3A, B). This suggests a more distal source and provenance from the north for the continental Upper
370 Gazimur Fm. deposits.

371 The evolution of the source area and depositional facies of the Jurassic sediments in the
372 East Transbaikalia Basin reflects the timing and dynamics of switch from marine to continental
373 depositional environment in the East Transbaikalia region. During the deposition of the marine
374 formations, the facies associations indicate proximal depositional environments to the south in the
375 Algachi-Kalgan zone evolving northward to distal environments in the Onon-Gazimur zone (Figs.
376 3, 4). It should be noted, however, that even the more distal zone periodically received coarse-
377 grained material possibly as turbidites. This geography of the basin is coherent with zircon source
378 areas situated mainly on the Erguna block. Based on facies associations, a shift in basin polarity
379 occurred with the deposition of the Upper Gazimur Fm. and may have initiated during the
380 deposition of the Kavykuchinsky Fm. By that time, the proximal zone was situated to the north in
381 the Onon-Gazimur region while the Algachi-Kalgan region became more distal. This shift in basin
382 polarity is consistent with the shift in detrital zircon provenance from the Erguna block to the
383 Selenga-Stanovoy Belt and Onon block as well as with the change from marine to continental
384 depositional environments.

385

386 **4.3. Closure of the Mongol-Okhotsk Ocean and tectonic position of the East**
387 **Transbaikalia Basin**

389 The new chronostratigraphy discussed above for the marine and continental deposits of the
390 East Transbaikalia Basin suggests that, in that region, the final marine regression occurred ~20 Ma
391 later than in Dzhagdy region (Sorokin et al., 2020). To the west, in the Western Transbaikalia
392 region, the closure of the Mongol-Okhotsk Ocean seems to have occurred earlier than in the east.
393 Detrital zircon U-Pb ages and Sm-Nd data from Early–Middle Jurassic sediments in the Irkutsk
394 Basin (southern margin of the Siberian Craton, Fig. 1) showed that the sediment input from
395 Transbaikalia began at the Early–Middle Jurassic boundary (Demonterova et al., 2017). A U-Pb
396 zircon age of 178.3 ± 5.0 Ma was obtained from a volcanic ash interlayer within the youngest
397 formation of the Irkutsk Basin in which detrital zircon grains of Transbaikalian provenance were
398 found (Mikheeva, 2017). These data indicate uplift and volcanic activity in Western Transbaikalia
399 that were interpreted as linked to an orogenic event related to the closure of the Mongol-Okhotsk
400 Ocean and the onset of continental collision (Demonterova et al., 2017; Arzhannikova et al., 2020).

401 Within the northern Argun-Idemeg terrane, an Oxfordian–Kimmeridgian final marine
402 regression in the East Transbaikalia Basin would slightly precede the Kimmeridgian–Tithonian
403 end of marine sedimentation suggested in the western Upper Amur Basin, itself preceding the
404 Berriasian–Valanginian marine regression in the northeastern Upper Amur Basin (Guo et al.,
405 2017). The segment of the Mongol-Okhotsk Belt extending from the East Transbaikalia Basin to
406 the Upper Amur Basin thus underwent progressive northeastward shift from marine to continental
407 sedimentation from the Oxfordian to the Valanginian, though being long-delayed when compared
408 to more westerly and easterly segments (Fig. 9A–C). Although this late regression should be
409 further documented, the delay may be due to the initial shape of paleo continental margins.

410 While the western and eastern segments of the Mongol-Okhotsk Ocean had already closed,
411 and the corresponding area passed into the orogenic stage of development with continental
412 sedimentation, the northern part of the Argun-Idemeg terrane underwent marine transgression.

413 marine environments persisted here from the late middle Jurassic to the Early Cretaceous,
414 successively being replaced by continental molasses.

415 Cawood et al. (2012) demonstrated that the age distribution of detrital zircons is partially
416 controlled by transport processes that reflect the tectonic setting of the basin they were deposited
417 in. Convergent margin basins contain a high proportion of detrital zircons with ages close to the
418 deposition age. Basins formed during continental collision (e.g., foreland basins) usually contain
419 zircons with a wider range of age distributions. Extensional basins are dominated by detrital
420 zircons, which ages are much older than the time of sedimentation (Cawood et al., 2012). The
421 detrital zircons within the East Transbaikalia Basin formations provide evidence of deposition in
422 convergence to collisional settings (Fig. 10). The marine Akatui, Bazanov, Bokhtin and
423 Sivachinsky fms. are dominated by detrital zircons with crystallization ages (CA) that are close to
424 their depositional ages (DA). Within the Akatui Fm. sample 78% of the zircon population have
425 $CA-DA < 100$ Ma. Within the Bazanov, Bokhtin and Sivachinsky fms. of 68%, 92% and 63%,
426 respectively which is consistent with deposition in a convergent setting. In comparison, the detrital
427 zircons from the continental Upper Gazimur Fm. have $CA-DA$ values that are indicative of
428 deposition in a collisional setting (29% of the zircon population within this sample have $CA-DA$
429 < 100 Ma). This indicates that detrital zircon age distribution patterns changed during the transition
430 from marine to continental deposits, reflecting a change in detrital zircon provenance described
431 above.

432 The deposition of marine sediments on the basement of the Argun-Idemeg terrane indicates
433 a collisional setting rather than a subduction one. The upward coarsening and several km-thick
434 successions of the East Transbaikalia Jurassic fms., punctuated in its lower part by a major
435 erosional unconformity (upper Jurassic deposits of the Onon-Gazimur and Algachi-Kalgan zones
436 overlap the Carboniferous and Devonian marine deposits, respectively (Fig. 4)) correspond to a
437 typical stratigraphic pattern of a foreland basin (De Celles, 2012). Sedimentological studies of Late
438 Cenozoic Himalayan peripheral foreland basin described the synorogenic sedimentation under

439 various depositional environments from marine-transitional to fluvial facies (Landon, 1991;
440 Burbank et al., 1996; Raiverman, 2002). The Siwalik continental molasse overlies the pre-Siwalik
441 marine deposits (Subathu Fm.) with an unconformity. The Subathu Fm. is composed of shallow
442 marine facies and consists of mudstone, sandstone and limestone (Najman et al., 2004). These
443 deposits are similar to the marine sediments of the Onon-Gazimur distal environment zone in the
444 East Transbaikalia Basin (Fig. 4). At the same time, in the Algachi-Kalgan zone, fine-grained
445 sediments were interbedded with conglomerates, which indicates coastal marine sedimentation.
446 The Upper Gazimur Fm., in places unconformably overlying marine sediments, may be an
447 analogue of the Siwalik continental molasse, which represents coarsening upward successions
448 from mudstone–sandstone to conglomerate facies (Kumar et al., 2011 and references therein).
449 Thus, we propose that by ~165–155 Ma, flexure of the northern Argun-Idemeg terrane formed a
450 peripheral foreland basin and resulted in marine transgression and sedimentation on the Paleozoic
451 terrane basement (Fig. 9D). The beginning of the foreland basin subsidence indicates the beginning
452 of the collision (Lin et al., 2017). Thus, the collision in Eastern Transbaikalia began about 165
453 million years ago, with a significant delay compared to the more western and eastern segments.
454 The reasons for this delay have not yet been clarified but we assume that it may be associated with
455 the original shape of the paleocontinental margins. Between ~158 Ma and ~155 Ma, the marine
456 basin was inverted in East Transbaikalia and turned into a continental foreland basin (Fig. 9E).
457 Marine sedimentation continued in the Upper Amur Basin until the Late Valanginian, and
458 complete disappearance of the marine depositional environments occurred by ~136–133 Ma (Guo
459 et al., 2017).

460 The inversion of the East Transbaikalia Basin was accompanied by syn-orogenic tectonic
461 deformation (Starchenko, 2010). The marine sediments of the East Transbaikalia were deeply
462 folded and dissected by reverse and thrust faults. The continental deposits of the Upper Gazimur
463 Fm. are conformable with respect to the folds of the Jurassic marine deposits, but form gentle
464 folds. Large thrusts deform the marginal parts of the basin. The contact is characterized by zones

465 or ultramylonites and breccias up to many hundreds of meters thick and intense tectono-
466 metamorphism. The dip of the thrusts is predominantly to the north and northwest. Late Jurassic
467 intrusions in some places intersect the thrusts and are not affected, limiting the time of thrusting
468 to the Late Jurassic (Starchenko, 2010).

469 Finally, it should be noted that this portion of the suture zone is the only one that does not
470 include a wide, clearly expressed Mongol-Okhotsk Belt. West of the East Transbaikalia Basin, the
471 suture zone appears double, surrounding the Onon Block. This double subduction is generally
472 documented as being double verging based on the apparent absence of strong collision event
473 between Mongolia and Siberia, although our study does not bring any argument to this model
474 (Wang et al., 2015; Daoudene et al., 2017; Sorokin et al., 2020). However, a double subduction could
475 explain the complete closure of the oceanic domain and formation of a more restricted collision belt
476 (Daoudene et al., 2017).

477

478 **5. Conclusions**

479

480 U-Pb (LA-ICP-MS) dating of detrital zircon from Jurassic marine and continental
481 sediments collected from the East Transbaikalia Basin allow for better constrains on the
482 stratigraphic framework of the deposits associated with the final closure of the Mongol-Okhotsk
483 Ocean. The initiation of the East Transbaikalia Basin took place in the Middle Jurassic as a
484 collisional foreland basin rather than in the Early Jurassic, as previously assumed. In the northern
485 Argun-Idemeg terrane region, the disappearance of the marine environments was diachronous
486 from Oxfordian in the western part of the East Transbaikalia Basin, to Late Valanginian NE of the
487 Upper Amur Basin. The northern Argun-Idemeg terrane was the last to collide with the Siberian
488 continent with a 5–10 million-years delay compared to the adjacent southwestern and northeastern
489 regions. This fact does not correspond to the widely supported scissor-like model of the Mongol-
490 Okhotsk Ocean closure, but testifies to its segmental closure. The geodynamic mechanism that led

491 to the delay in collision of the northern Argun-Idemeg terrane must be further documented but
492 could be related to the peculiar double-verging subduction setting inferred for this segment of the
493 Mongol-Okhotsk suture zone or to the peculiar shape of the paleo continental margins.

494

495 **Acknowledgments:**

496 The study was conducted in the frame of the grant of the Ministry of Science and High Education
497 of the Russian Federation No. 075-15-2019-1883. Detrital zircons were extracted from the bulk
498 samples and prepared for U-Pb analysis at the Centre for Geodynamics and Geochronology of the
499 Institute of the Earth's Crust SB RAS (Irkutsk, Russia). U-Pb isotope analysis of zircons was made
500 at the Analytical Centre of mineralogical, geochemical and isotope Studies at the Geological
501 Institute, SB RAS (Ulan-Ude, Russia). We thank three anonymous reviewers for their valuable
502 comments, which greatly improved the original manuscript.

503

504 **References**

505

- 506 Arzhannikova, A.V., Demonterova, E.I., Jolivet, M., Arzhannikov, S.G., Mikheeva, E.A., Ivanov,
507 A.V., Khubanov, V.B., Pavlova, L.A., 2020. Late Mesozoic topographic evolution of
508 western Transbaikalia: Evidence for rapid geodynamic changes from the Mongol-Okhotsk
509 collision to widespread rifting. *Geosci. Front.* 11, 1695-1709.
- 510 Black, L.P., Kamo, C.L., Allen, C.M., Aleinikoff, J.N., Davis, D.W., Korsch, R.J., Foudoulis,
511 C., 2003. TEMORA 1: a new zircon standard for Phanerozoic U–Pb geochronology.
512 *Chem. Geol.* 200, 155–170.
- 513 Burbank, D.W., Beck, R.A., Mulder, T., 1996. The Himalayan foreland basin. In: Yin, A., Harrison,
514 T.M. (Eds.), *Tectonic Evolution of Asia*. Cambridge Univ. Press, USA, pp. 149 –188.
- 515 Buyantuev, M. D., Khubanov, V. B. and Vrublevsckaya, T. T., 2017. U-Pb LA-ICP-MS dating of
516 zircons from subvolcanics of the bimodal dyke series of the Western Transbaikalia:

- 517 technique, and evidence of the Late Paleozoic extension of the crust. *Geodyn. Tectonophys.*
518 8(2), 369-384 (in Russian).
- 519 Cawood, P.A., Hawkesworth, C.J., Dhuime, B., 2012. Detrital zircon record and tectonic setting.
520 *Geology* 40 (10), 875–878.
- 521 Chaban, N.N., 2002. Geological map of scale 1:200 000, sheet M-50-X. VSEGEI, St.-Peterburg.
- 522 Cogné, J.-P., Kravchinsky, V.A., Halim, N., Hankard F., 2005. Late Jurassic-early Cretaceous
523 closure of the Mongol-Okhotsk Ocean demonstrated by new Mesozoic palaeomagnetic
524 results from Trans-Baikal area (SE Siberia). *Geophys. J. Int.* 163, 813-832.
- 525 Daoudene, Y., Gapais, D., Cogné, J-P. & Ruffet, G., 2017. Late Mesozoic continental extension in
526 northeast Asia – Relationship to plate kinematics. *BSGF-Earth Sciences Bulletin* 188, 1-2,
527 10.
- 528 Darby, B.J., Davis, G.A., Zheng, Y., 2001. Structural evolution of the southwestern Daqing Shan,
529 Yinshan belt, Inner Mongolia, China. In: Hendrix, M.S., Davis, G.A. (Eds.), *Paleozoic and*
530 *Mesozoic tectonic evolution of central Asia: From continental assembly to intracontinental*
531 *deformation*. *Geol. Soc. Am. Bull. Memoirs*, Boulder, Colorado, 194, pp. 199-214.
- 532 Davis, G.A., Cong, W., Yadong, Z., Jinjiang, Z., Changhou, Z., and Gehrels, G.E., 1998. The
533 enigmatic Yinshan fold-and-thrust belt of northern China: New views on its intraplate
534 contractional styles. *Geology* 26, 43-46.
- 535 De Celles, P.G., 2012. Foreland basin systems revisited: variations in response to tectonic settings.
536 In: Busby, C., Azor, A. (Eds.), *Tectonics of Sedimentary Basins: Recent Advances*. John
537 Wiley and Sons publisher, pp. 405-426.
- 538 Demonterova, E.I., Ivanov, A.V., Mikheeva, E.A., Arzhannikova, A.V., Frolov, A.O., Arzhannikov,
539 S.G., Bryanskiy, N.V., Pavlova, L.A., 2017. Early to Middle Jurassic history of the
540 southern Siberian continent (Transbaikalia) recorded in sediments of the Siberian Craton:
541 Sm-Nd and U-Pb provenance study. *Bull. Soc. Géol. Fr.* 188, 1-2 (8).

- 542 Dickinson, W.R., Genreis, G.E., 2009. Use of U-Pb ages of detrital zircons to infer maximum
543 depositional ages of strata: A test against a Colorado Plateau Mesozoic database. *Earth
544 Planet. Sci. Lett.* 288, 115–125. doi:10.1016/j.epsl.2009.09.013.
- 545 Didenko, A.N., Efimov, A.S., Nelyubov, P.A., Sal'nikov, A.S., Starosel'tsev, V.S.,
546 Shevchenko, B.F., Goroshko, M.V., Gur'yanov, V.A., Zamozhnyaya, N.G., 2013.
547 Structure and evolution of the Earth's crust in the region of junction of the Central Asian
548 Fold Belt and the Siberian Platform: Skovorodino–Tommot profile. *Russ. Geol. Geophys.*
549 54, 1236–1249.
- 550 Donskaya, T.V., Gladkochub, D.P., Mazukabzov, A.M., & Ivanov, A.V., 2013. Late Paleozoic-
551 Mesozoic subduction-related magmatism at the southern margin of the Siberian continent
552 and the 150 million-year history of the Mongol-Okhotsk Ocean. *J. Asian Earth Sci.* 62, 79-
553 97.
- 554 Gordienko, I. V. and Kuz'min, M. I., 1999. Geodynamics and metallogeny of the Mongolo-
555 Transbaikalian region. *Russ. Geol. Geophys.* 40, 11, 1545-1562 (in Russian).
- 556 Gordienko, I.V., Metelkin, D.V., and Vetluzhskikh, L.I., 2019. The Structure of the Mongol-
557 Okhotsk Fold Belt and the Problem of Recognition of the Amur Microcontinent. *Russ.
558 Geol. Geophys.* 60, 3, 267-286.
- 559 Griffin, W.L., Powell, W.J., Pearson, N.J., O'Reilly, S.Y., 2008. GLITTER: Data reduction software
560 for laser ablation ICP–MS. In: Sylvester, P.J. (Ed.), *Laser Ablation ICP-MS in the Earth
561 Sciences*. MAC Short-Course series Association, 40, 307-311.
- 562 Guo, Z.H., Yang, Y.T., Zhabrev, S., Hou, Z.H., 2017. Tectonostratigraphic evolution of the
563 Mohe-Upper Amur Basin reflects the final closure of the Mongol-Okhotsk Ocean in
564 the latest Jurassic–earliest Cretaceous. *J. Asian Earth Sci.* 145 (B), 494 –511.
- 565 Halim, N., Kravchinsky, V., Gilder, S., Cogne J.-P., Alexyutin M., Sorokin A., Courtillot V., Chen,
566 Y., 1998. Palaeomagnetic study from the Mongol-Okhotsk region: rotated Early

- 567 Cretaceous volcanics and remagnetized Mesozoic sediments. *Earth Planet. Sci. Lett.*, 159,
568 133-145.
- 569 Ivanov, A.V., Demonterova, E.I., He, H.Y., Perepelov, A.B., Travin, A.V., Lebedev, V.A., 2015.
570 Volcanism in the Baikal rift: 40 years of active-versus-passive model discussion. *Earth Sci*
571 *Rev.* 148, 18-43. doi: 10.1016/j.earscirev.2015.05.011.
- 572 Jackson, S. E., Pearson, N. J., Griffin, W. L. and Belousova, E. A., 2004. The application of laser
573 ablation-inductively coupled plasma-mass spectrometry to in situ U–Pb zircon
574 geochronology. *Chem. Geol.* 211, 47-69.
- 575 Jolivet, M., Arzhannikova, A., Frolov, A., Arzhannikov, S., Kulagina, N., Akulova, V., Vassallo,
576 R., 2017. Late Jurassic – Early Cretaceous paleoenvironment evolution of the Transbaikalian
577 basins (SE Siberia): implications for the Mongol-Okhotsk orogeny. *Bull. Soc. geol. Fr.*
578 188, 1-2, 9. DOI: 10.1051/bsgf/2017010
- 579 Karsakov, L.P., Chzhao, Ch. Malyshev, Ju.F., Gorshko, M.V., 2005. Tectonics, deep structure and
580 metallogeny of the junction area between the Central Asian and Pacific belts. Explanatory
581 note to the 1:500000-scale tectonic map. FEB RAS, Vladivostok, Khabarovsk, 264 pp. (in
582 Russian).
- 583 Khlif, N., Sasim, S. A. and Andreeva, U. S., 2017. Elemental features and petrogenesis of the
584 volcanic rocks of the Kailassk and Turginsk suites of the Alexandrovo-Zavodsk
585 depression, south-east Transbaikalian area. *The Bulletin of Irkutsk State University. Series*
586 *Earth Sciences* 19, 108-129 (in Russian).
- 587 Khubanov, V. B., Buyantuev, M. D., and Tsygankov, A. A., 2016. U-Pb dating of zircons from
588 PZ(3)-MZ igneous complexes of Transbaikalia by sector-field mass spectrometry with
589 laser sampling: technique and comparison with SHRIMP. *Russ. Geol. Geophys.* 57(1),
590 190-205.

- 591 Kravchinsky, V.A., Cogne, J.-P., Harbert, W.P. and Kuzmin, M.I., 2002. Evolution of the Mongol–
592 Okhotsk Ocean as constrained by new palaeomagnetic data from the Mongol–Okhotsk
593 suture zone, Siberia. *Geophys. J. Int.* 148, 34–57.
- 594 Kumar, R., Ghosh, S.K., Sangode, S.J., 2011. Sedimentary architecture of late Cenozoic Himalayan
595 foreland basin fill: An overview. *Memoir Geological Society of India* 78, 245-280.
- 596 Kuzmin, M. I., and Kravchinsky, V. A., 1996. First paleomagnetic data for Mongol-Okhotsk fold
597 belt. *Russ. Geol. Geophys.* 37, 1, 54-62 (in Russian).
- 598 Kuzmin, M.I., and Filippova, I.B., 1979. Middle–Late Paleozoic and Mesozoic development of the
599 Mongol-Okhotsk belt. In: Zonnenshain, L.P. Sorokhtin, O.G. (Eds.), *Structure of the*
600 *lithospheric plates (interaction of plates and formation of crustal structures)*. IO AS,
601 Moscow, pp. 189-226 (in Russian).
- 602 Lin, D., Satybaev, M., FuLong, C., HouQi, W., PeiPing, S., WeiQiang, J., Qiang, X., LiYun, Z.,
603 Qasim, M., Baral, U., 2017. Processes of initial collision and suturing between India and
604 Asia. *Sci. China Earth Sci.* 60, 635–651.
- 605 Liu, H., Li, Y., Wan, Z., Lai, C.-K., 2020. Early Neoproterozoic tectonic evolution of the Erguna
606 Terrane (NE China) and its paleogeographic location in Rodinia supercontinent: Insights
607 from magmatic and sedimentary record. *Gondwana Res.* 88, 185–200.
- 608 Metelkin, D.V., Vernikovskiy, V.A., Kazansky, A.Y., Wingate, M.T.D., 2010. Late Mesozoic
609 tectonics of Central Asia based on paleomagnetic evidence. *Gondwana Res.* 18, 400-419.
- 610 Metelkin, D.V., Gordienko, I.V., Klimuk, V.S., 2007. Paleomagnetism of Upper Jurassic basalts
611 from Transbaikalia: new data on the time of closure of the Mongol-Okhotsk Ocean and
612 Mesozoic intraplate tectonics of Central Asia. *Russ. Geol. Geophys.* 48, 10, 825-834.
- 613 Mikheeva, E.A., 2017. Age limits, correlation, source areas of the Jurassic deposits in the Irkutsk
614 Basin: Abstracts of M.S. Thesis, IEC SB RAS, Irkutsk, 16 pp. (in Russian).
- 615 Najman, Y., Johnson, K., White, N., Olivers, G., 2004. Evolution of Himalayan foreland basin, NW
616 India. *Basin Res.* 16, 1-24.

- 617 Nie, S., 1991. Paleoclimatic and paleomagnetic constraints on the Paleozoic reconstructions of
618 south China, north China and Tarim. *Tectonophysics* 196, 279–308.
- 619 Nie, S., Rowley, D.B., Ziegler, A.M., 1990. Constraints on the location of Asian microcontinents in
620 Paleo-Tethys during Late Palaeozoic. In: McKerrow, W.S., Scotese, C.R. (Eds.),
621 Palaeozoic Palaeogeography and Biogeography. *Geol. Soc. Mem. Am.* 12, 12397–12409.
- 622 Parfenov, L.M., Berzin, N.A., Badarch, G., Belichenko, V.G., Bulgatov, A.N., Dril, S.I., Khanchuk,
623 A.I., Kirillova, G.L., Kuz'min, M.I., Nokleberg, W.J., Ogasawara, M., Obolenskiy, A.A.,
624 Prokopiev, A.V., Rodionov, S.M., Scotese, C.R., Timofeev, V.F., Tomurtogoo, O., Yan,
625 H., 2010. Tectonic and metallogenic model for northeast Asia. In: Nokleberg, W.J. (Ed.),
626 Metallogensis and tectonics of northeast Asia. *U.S. Geol. Surv. Prof. Pap.* 1765, Chapter
627 9, 56 pp.
- 628 Parfenov, L.M., Berzin, N.A., Khanchuk, A.I., Badarch, G., Belichenko, V.G., Bulgatov, A.N.,
629 Dril', S.I., Kirillova, G.L., Kuzmin, M.I., Nockleberg, W., Prokopyev, A.V., Timofeev,
630 V.F., Tomurtogoo, O. and Yan, X., 2003. A model for the formation of orogenic belts in
631 Central and NE Asia. *Russ. J. Pacific Geol.* 22, 6, 7–41 (in Russian).
- 632 Parfenov, L.M., Popeko, L.I. and Tomurtogo, O., 1999. The problems of tectonics of the Mongol-
633 Okhotsk orogeny. *Russ. J. Pacific Geol.* 18, 5, 24-43 (in Russian)
- 634 Raiverman, V., 2002. Foreland Sedimentation in Himalayan Tectonic Regime - A relook at the
635 orogenic process, Bisen Singh Mahendra Pal Singh Publishers, Dehra Dun, 371 pp.
- 636 Rossignol, C., Hallot, E., Bourquin, S., Poujol, M., Jolivet, M., Pellenard, P., Ducassou, C., Nalpas,
637 T., Heilbronn, G., Yu, J., Dabard, M.-P., 2019. Using volcanoclastic rocks to constrain
638 sedimentation ages: To what extent are volcanism and sedimentation synchronous?
639 *Sediment. Geol.* 381, 46–64.
- 640 Sasim, S.A., Dril, S.I., Travin, A.V., Vladimirova, T.A., Gerasimov, N.S., Noskova, Y.V., 2016.
641 Shoshonite-latitude series of the Eastern Transbaikalia: $^{40}\text{Ar}/^{39}\text{Ar}$ age, geochemistry, and

- 642 Sr-IND isotope composition of rocks from the Akatui volcano-plutonic association of the
643 Aleksandrovskii Zavod depression. *Russ. Geol. Geophys.* 57, 5, 756-772.
- 644 Scotese, C.R., 1991. Jurassic and Cretaceous plate tectonic reconstruction. *Palaeogeogr.*
645 *Palaeoclimatol. Palaeoecol.* 87, 493–501.
- 646 Sengör, A.M.C., Natal'in, B.A., 1996. Paleotectonics of Asia: fragments of a synthesis. In: Yin, A.,
647 Harrison, T.M. (Eds.), *The Tectonics of Asia*. Cambridge Univ. Press, New York, pp. 486–
648 640.
- 649 Sláma, J., Košler, J., Condon, D.J., Crowley, J.L., Gerdes, A., Hanchar, J.M., Horstwood, M.S.A.,
650 Morris, G.A., Nasdala, L., Norberg, N., Schaltegger, U., Schoene, B., Tubrett, M.N.,
651 Whitehouse, M.J., 2008. Plesovice zircon - A new natural reference material for U-Pb and
652 Hf isotopic microanalysis. *Chem. Geol.* 249, 1–35.
- 653 Smirnova, Y.N. Sorokin, A.A., 2019. Age and depositional settings of the Ordovician Chalovskaya
654 group in the Argun massif, eastern part of the Central Asian Fold Belt. *Stratigr. Geol.*
655 *Correl.* 27, 3, 277-296.
- 656 Sorokin, A. A., Zaika, V.A., Kovach, V.P., Kotov, A.B., Xu, W., Yang, H., 2020. Timing of closure
657 of the eastern Mongol – Okhotsk Ocean: Constraints from U – Pb and Hf isotopic data of
658 detrital zircons from metasediments along the Dzhagdy Transect. *Gondwana Res.* 81, 58 –
659 78. <https://doi.org/10.1016/j.gr.2019.11.009>
- 660 Starchenko V.V., 2006. Geological map of scale 1:200000, sheet M-50-XI. VSEGEI, St.-Peterburg
661 (in Russian).
- 662 Starchenko V.V. (ed.), 2010. State Geological Map of the Russian Federation. Scale 1:1000000.
663 Sheet M-50 Borzya. Explanatory note. VSEGEI, Saint-Petersburg, 553 pp (in Russian).
- 664 Sun, Ch., Xu, W., Cawood, P.A., Tang, J., Zhao, Sh., Li, Y., Zhang, X., 2019. Crustal growth and
665 reworking: A case study from the Erguna Massif, eastern Central Asian Orogenic Belt. *Sci.*
666 *Rep.* 9, 17671. <https://doi.org/10.1038/s41598-019-54230-x>

- 667 Sun, D.Y., Gou, J., Wang, T.H., Ren, Y.S., Liu, Y.J., Guo, H.Y., Liu, X.M., Hu, Z.C., 2013.
668 Geochronological and geochemical constraints on the Erguna massif basement, NE China
669 - subduction history of the Mongol – Okhotsk oceanic crust. *Int. Geol. Rev.* 55, 14, 1801 –
670 1816. <https://doi.org/10.1080/00206814.2013.804664>.
- 671 Tandon, S.K., 1991. The Himalayan Foreland: focus on Siwalik Basin. In: Tandon, S.K., Pant, C.C.,
672 Casshyap, S.M. (Eds.), *Sedimentary Basins of India: Tectonic Context*, Gyanodaya
673 Prakashan, Nainital (India), pp. 177– 201.
- 674 Tauson, L.V., Antipin, V.S., Zakharov, M.N. and Zubkov, V.S., 1984. Geochemistry of the
675 Mesozoic latites of Transbaikalia. Nauka, Novosibirsk, 205 pp. (in Russian).
- 676 Tomurtogoo, O., Windley, B.F., Kroner, A., Badarch, G., and Liu, D.Y., 2005. Zircon age and
677 occurrence of the Adaatsag ophiolite and Muron shear zone, central Mongolia: Constraints
678 on the evolution of the Mongol-Okhotsk Ocean, suture and orogeny. *J. Geol. Soc. London*
679 162, 197–229.
- 680 Troshin, Yu.P., 1978. Geochemistry of volatile components in magmatic rocks, areolas and ores of
681 East Transbaikalia. Nauka, Novosibirsk, 165 pp. (in Russian).
- 682 Van der Voo, R., Van Hinsbergen, D.J.J., Domeier, M., Spakman, W., and Torsvik, T.H., 2015.
683 Latest Jurassic–earliest Cretaceous closure of the Mongol-Okhotsk Ocean: A
684 paleomagnetic and seismological-tomographic analysis. In: Anderson, T.H., Didenko,
685 A.N., Johnson, C.L., Khanchuk, A.I., and MacDonald, J.H., Jr. (Eds.), *Late Jurassic Margin*
686 *of Laurasia - A Record of Faulting Accommodating Plate Rotation*. *Geol. Soc. Am. Spec.*
687 *Pap.* 513, pp. 1–18. [https://doi.org/10.1130/2015.2513\(19\)](https://doi.org/10.1130/2015.2513(19)).
- 688 Vermeesch, P., 2012. On the visualisation of detrital age distributions. *Chem. Geol.* 312, 190-194.
- 689 Vermeesch, P., 2018. IsoplotR: a free and open toolbox for geochronology. *Geosci. Front.* 9, 1479-
690 1493. <https://doi.org/10.1016/j.gsf.2018.04.001>.
- 691 Wang, W., Tang, J., Xu, W.-L., Wang, F., 2015. Geochronology and geochemistry of Early Jurassic
692 volcanic rocks in the Erguna Massif, northeast China: Petrogenesis and implications for

- 693 the tectonic evolution of the Mongol–Okhotsk suture belt. *Lithos* 218–219, 73–80.
- 694 Wiedenbeck, M., Allé, P., Corfu, F., Griffin, W.L., Meier, M., Oberli, F., Van Quadt, A., Roddick,
695 J.C., Spiegel, W., 1995. Three natural zircon standards for U-Th-Pb, Lu-Hf, trace element
696 and REE analyses. *Geostandards Newsletter* 19, 1–23.
- 697 Wu, F.-Y., Sun, D.-Y., Ge, W.-C., Zhang, Y.-B., Grant, M.L., Wilde, S.A., Jahn, B.-M., 2011.
698 Geochronology of the Phanerozoic granitoids in northeastern China. *J. Asian Earth Sci.* 41,
699 1–30.
- 700 Yang, Y.-T., Guo, Z.-X., Song, C.-C., Li, X.-B., He, S., 2015. A short-lived but significant Mongol
701 – Okhotsk collisional orogeny in latest Jurassic – earliest Cretaceous. *Gondwana Res.* 28,
702 1096-1116.
- 703 Yi, Z., Meert, J. G., 2020. A closure of the Mongol-Okhotsk Ocean by the
704 Middle Jurassic: Reconciliation of paleomagnetic and geological evidence. *Geophys. Res.*
705 *Lett.* 47, e2020GL088235. <https://doi.org/10.1029/2020GL088235>
- 706 Yin, A., Nie, S., 1996. A Phanerozoic plinstatic reconstruction of China and its neighboring regions.
707 In: Yin, A., Harrison, T.M. (Eds.), *The tectonic evolution of Asia*. Cambridge University
708 Press, Cambridge, pp. 442-485.
- 709 Yin, A., Nie, S., 1993. An indentation model for North and South China collision and the development
710 of the Tan Lu and Honam fault systems, eastern Asia. *Tectonics* 12, 801– 813.
- 711 Zakharov, M.N., 1972. Petrology and geochemistry of the Akatui effusive-intrusive complex in the
712 Priargun structural zone of East Transbaikalia: Abstracts of M.S. Thesis. Irkutsk, 22 pp. (in
713 Russian).
- 714 Zhao, X., Coe, R.S., Zhou, Y.X., Wu, H.R., Wang, J., 1990. New palaeomagnetic results from
715 northern China: collision and suturing with Siberia and Kazakhstan. *Tectonophysics* 181,
716 43–81.
- 717 Zonenshain, L.P., Kuzmin, M.I. & Natapov, L.M. 1990. *Geology of the USSR:*
718 *A Plate Tectonic Synthesis*. AGU, Geodynamics Series, 21.

719 Zorin, Yu.A. 1999. Geodynamics of the western part of the Mongolia–Okhotsk
720 collisional belt, Trans-Baikal region (Russia) and Mongolia. *Tectonophysics*, 306, 33–56.
721 Zorin, Yu.A., Belichenko, V.G., Turutanov, E.Kh., Kozhevnikov, V.M., Sklyarov, E.V.,
722 Tomurtogoo, O., Khosbayar, P., Arvisbaatar, N. and Byambaa, Ch., 1998. Terranes in East
723 Mongolia and Central Transbaikalia and evolution of the Okhotsk-Mongolian fold belt.
724 *Russ. Geol. Geophys.* 39, 1, 11-25 (in Russian).

725

726 **Figure captions:**

727 Fig. 1. Tectonic position of the Mongol-Okhotsk Belt (modified from Parfenov et al., 1999). The
728 location of the Mongol-Okhotsk suture (red line) is given after Tomurtogoo et al. (2005).

729

730 Fig. 2. Temporal-spacial distribution map of Phanerozoic granitoids in the Erguna block (modified
731 after Wu et al., 2011) with the addition of a sampling place of granodiorite and gneiss of
732 Paleoproterozoic age (after Sun et al., 2019).

733

734 Fig. 3. –(A) Geological map of the East Transbaikalia Basin and adjacent area simplified after
735 (Starchenko, 2010) with modification of the age of some geological units after (Sasim et
736 al., 2016; Gordienko et al., 2019). 1 – Quaternary alluvial deposits, 2 – Neogene lacustrine
737 sediments, 3 – Cretaceous sedimentary-volcanic deposits, 4 – Jurassic continental deposits,
738 5 – Jurassic marine deposits, 6 – Middle-Late Jurassic volcanic rocks, 7 – Permo-Triassic
739 sedimentary rocks, 8 – Permo-Triassic volcanic rocks, 9 – Devonian-Carboniferous
740 sedimentary-volcanic deposits and rhyolites, 10 – Ordovician-Silurian metamorphic
741 sedimentary-volcanic rocks; 11 – Early Paleozoic granitoids, 12 – Mezo- and
742 Neoproterozoic metamorphic sedimentary-volcanic rocks, 13 – Paleoproterozoic
743 metamorphic sedimentary rocks and granitoids. The bold black line shows main thrusts
744 along the Mongol-Okhotsk Suture, the white dotted line indicates the boundary between

745 the Onon-Gazimur (O-G) and Aigachi-Kaigan (A-K) zones. (B) Scheme of the tectonic
746 blocks in the study area with ages of magmatic rocks.

747 Fig. 4. Jurassic general stratigraphic section in the Est Transbaikalia Basin for distal (A) and
748 proximal (B) environment zones (after Chaban, 2002; Starchenko, 2006). 1 – breccias, 2 –
749 conglomerates, 3 – sandstones, 4 – siltstones, 5 – argillites, 6 – tuffs, 7 – dikes, 8 – remains
750 of fauna. Red points indicate samples position (schematically, without reference to depth
751 and upper/lower parts of fms.)

752

753 Fig. 5. Sedimentary sections in sampling places (A–E) and field views (A'-E') of the Akatui (A, A'),
754 Bazanov (B, B'), Bokhtin (C, C'), Sivachinsky (D) and Upper Gazimur (E, E') formations.
755 Red dots indicate sampling places. 1 – conglomerate, 2 – gritstone, 3 – sandstone, 4 –
756 siltstone, 5 – dike, 6 – cover (no data).

757

758 Fig. 6. U-Pb concordia diagrams and histograms coupled with kernel density estimates for zircons
759 from A – Akatui, B – Bazanov, C – Bokhtin, D – Sivachinsky, E – Upper Gazimur Fms. n
760 – numbers of data. The histograms, where there are no statistically significant populations
761 of zircons of Precambrian ages, show only zircons with Paleo- and Mesozoic ages.
762 Frequency histograms for detrital zircons were drawn using bin width of 20 Ma. The lilac
763 area is the kernel density estimates (Vermeesch, 2012; 2018) with bandwidth of 10 Ma.

764

765 Fig. 7. U-Pb concordia diagrams for zircon from samples Ln-15-40 (A) and Ln-15-48 (B). Black
766 ellipses are used to calculate the concordia age shown by red ellipse using IsoplotR
767 program (Vermeesch, 2018). Grey ellipses are omitted from the calculation. n - is the
768 number of considered individual analysis over the total numbers of data.

769

770 Fig. 8. Timing of marine and continental sedimentation in the Est Transbaikalia Basin.

771

772 Fig. 9. (A–C) Paleotectonic reconstructions for the Middle Jurassic–Early Cretaceous Mongol-
773 Okhotsk Ocean closure, (A) Callovian-Oxfordian, –(B) Kimmerigian, –(C) Valanginian. 1
774 – cratons, 2– collage of accreted terranes, 3 – Mesozoic basins: IB – Irkutsk Basin, ETB –
775 East Transbaikalia Basin, UAB – Upper Amur Basin, SAB – South Aldan Basin, HB –
776 Hailar Basin, SB - Songliao Basin, 4 – Mongol-Okhotsk belt, 5 – Mongol-Okhotsk suture
777 zone, 6 – subduction zone, 7 – normal faults, 8 – reverse faults, 9 – marine space, West
778 TSB – Western Transbaikalia, Dzh – Dzhagdy region. –(D–E) Models of the East
779 Transbaikalia Basin sedimentation for marine and continental environment, respectively. 1
780 – continental crust, 2 – mantle lithosphere, 3 – marine space, 4 – sediments.

781

782 Fig. 10. Tectonic setting diagram for detrital zircons from the marine and continental deposits of the
783 East Transbaikalia Basin (modified after Cawood et al., 2012). (A) orange field –
784 convergent settings, (B) blue field - collisional settings, (C) green field – extensional
785 settings. CA–DA: difference between the crystallization and depositional ages of the
786 zircons. Color lines show the age distribution of detrital zircons for the studied formations.

787

788 **Supplementary Data:**

789 Table S1. U-Pb analytical results of detrital zircon from the Akatui Fm. (sample Ln-15-24).

790 Table S2. U-Pb analytical results of detrital zircon from the Bazanov Fm. (sample Ln-15-16).

791 Table S3. U-Pb analytical results of magmatic zircon from the dikes intruding the Bokhtin (sample
792 Ln-15-40) and Upper Gazimur (sample Ln-15-48) Fms.

793 Table S4. U-Pb analytical results of detrital zircon from the Bokhtin Fm. (sample Ln-15-43).

794 Table S5. U-Pb analytical results of detrital zircon from the Sivachinsky Fm. (sample Ln-15-47).

795 Table S6. U-Pb analytical results of detrital zircon from the Upper Gazimur Fm. (sample Ln-15-9).

796

797

798

799

800

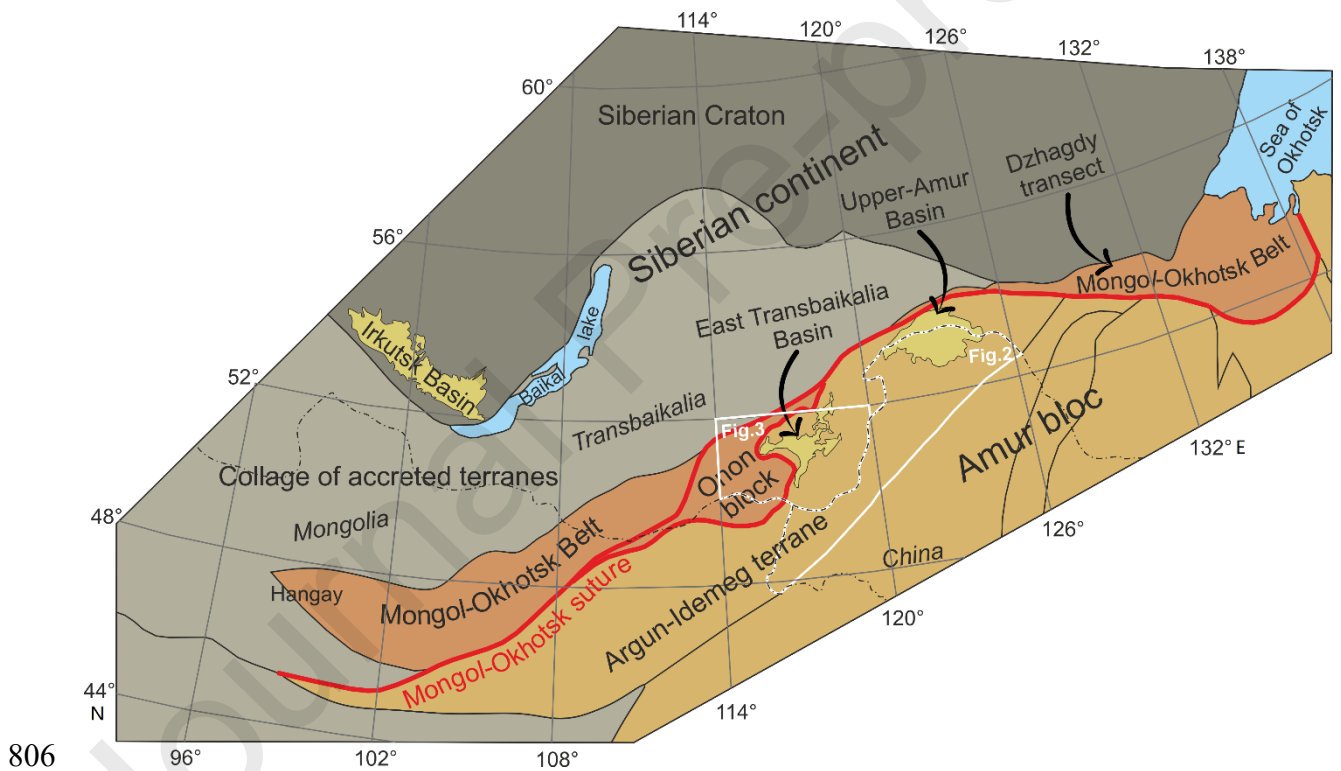
801 **Research highlights**

802• The closure of the Mongol-Okhotsk Ocean was not scissor-like, but segmental

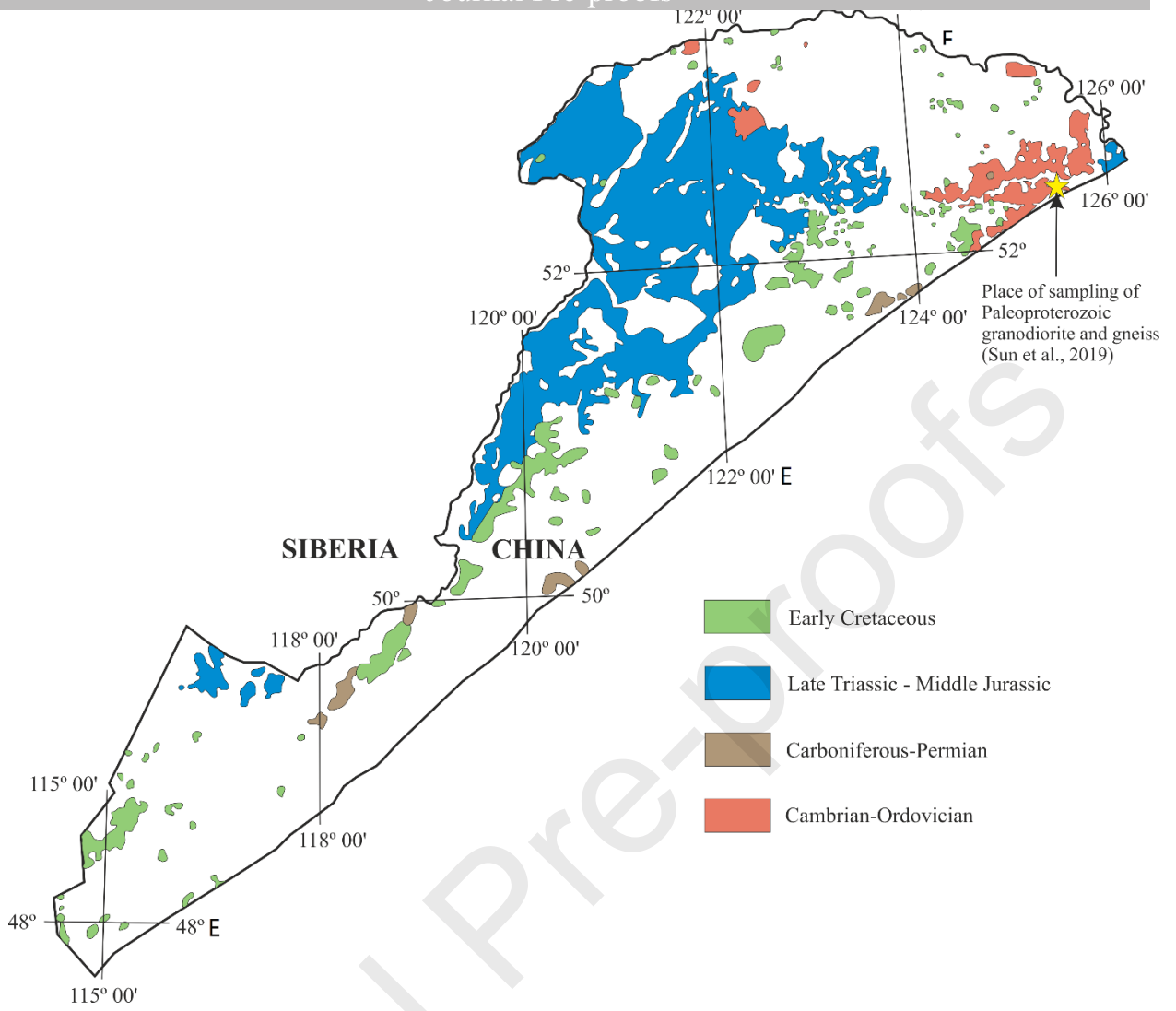
803• Northern Argun-Idemeg terrane was the last to be accreted to the Siberian continent

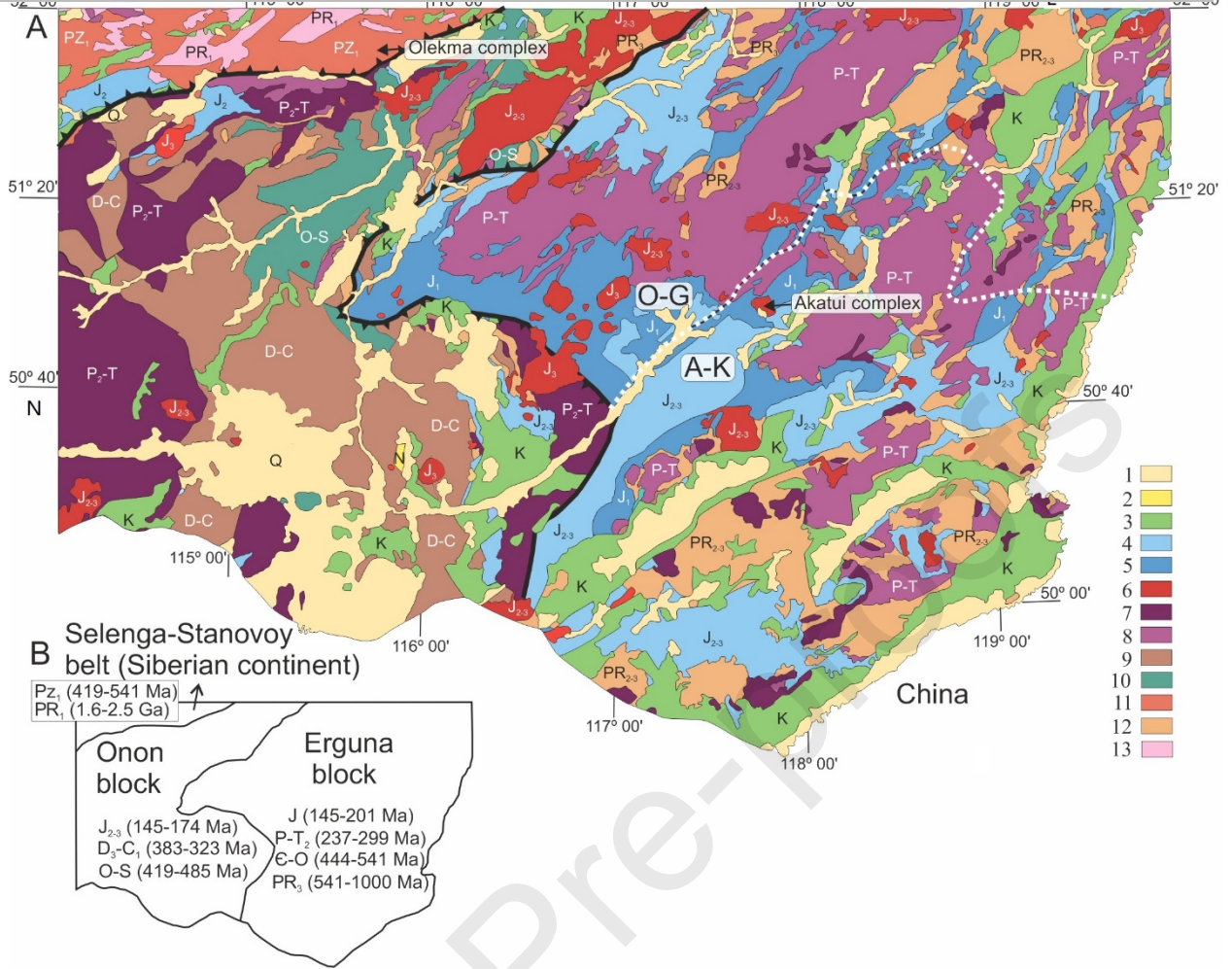
804• First U–Pb (LA-ICP-MS) detrital zircon ages for the marine and continental deposits

805

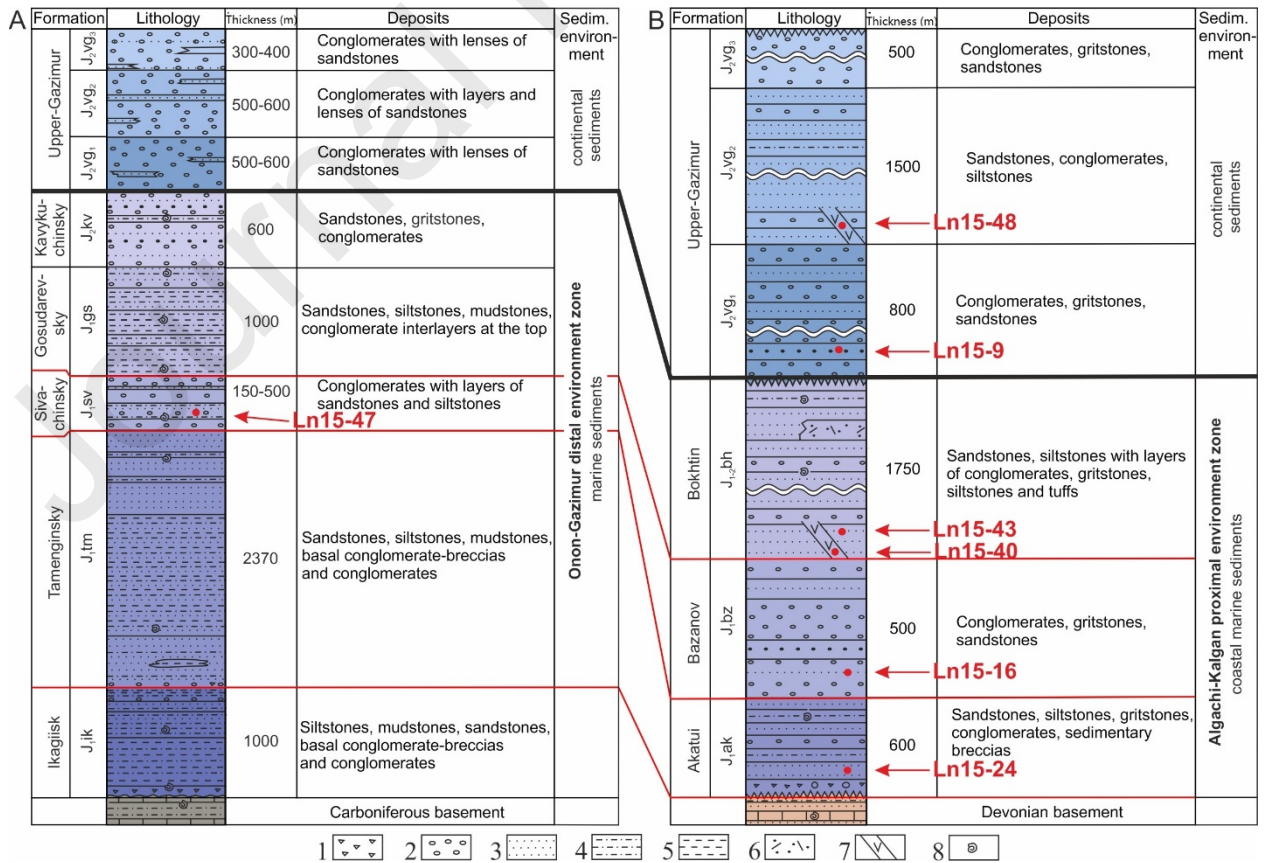


806

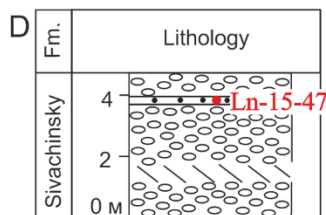
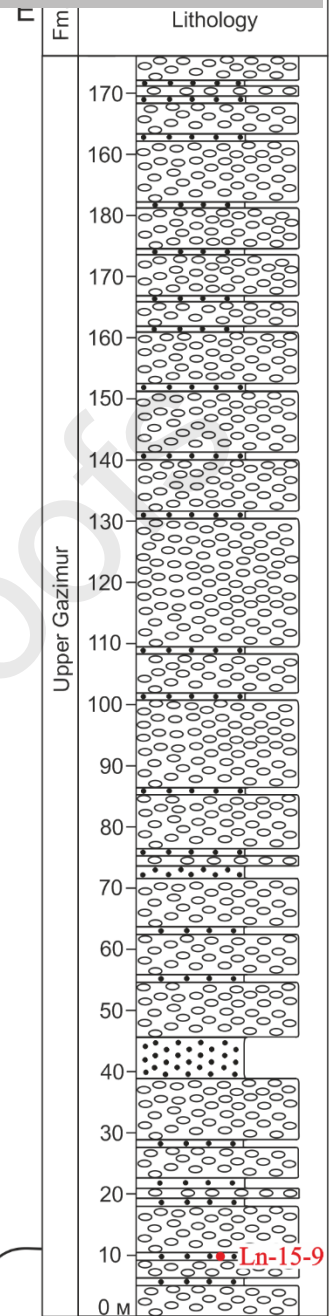
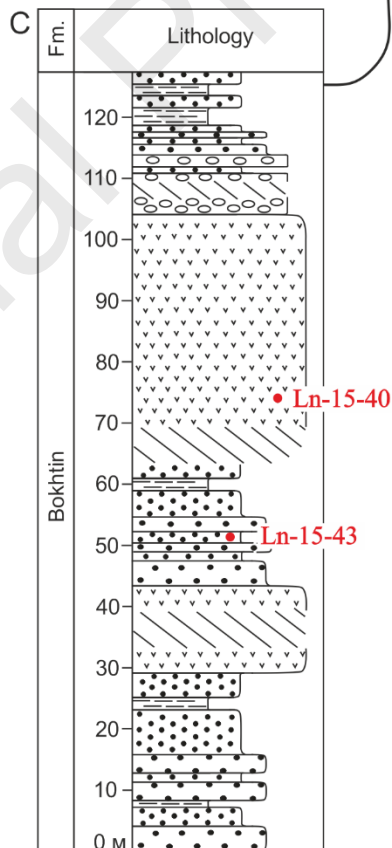
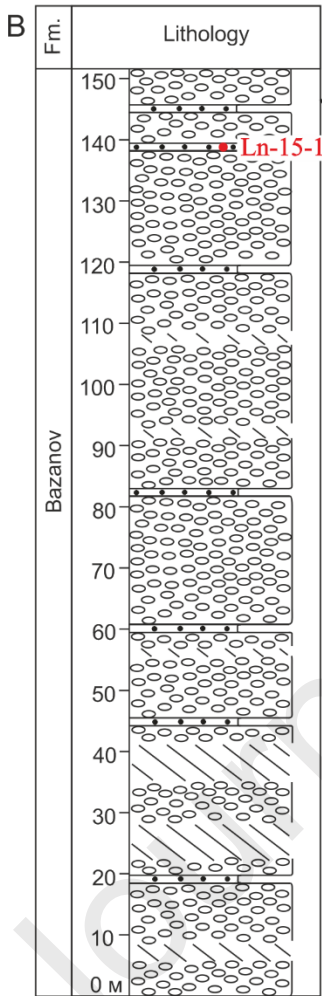
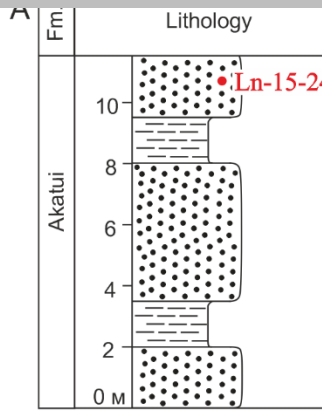


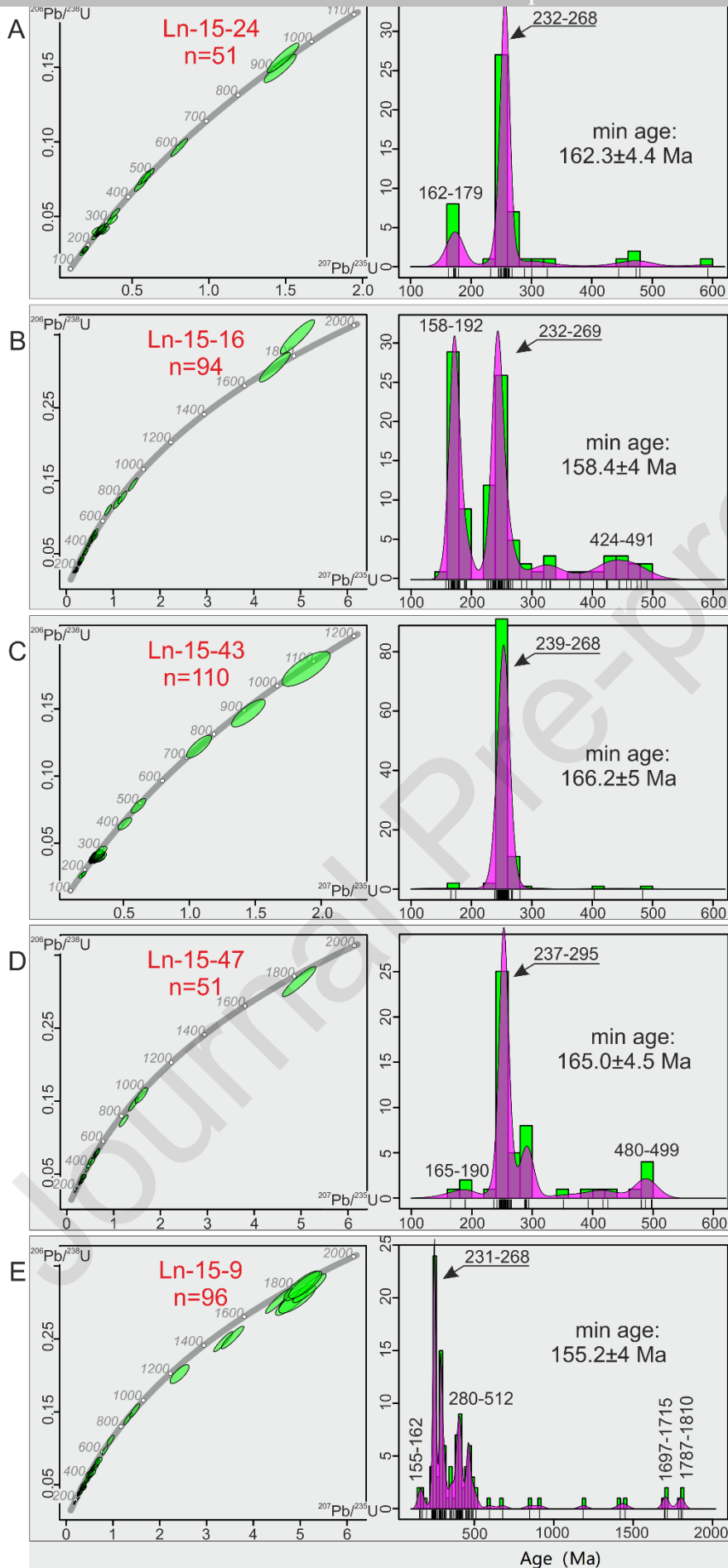


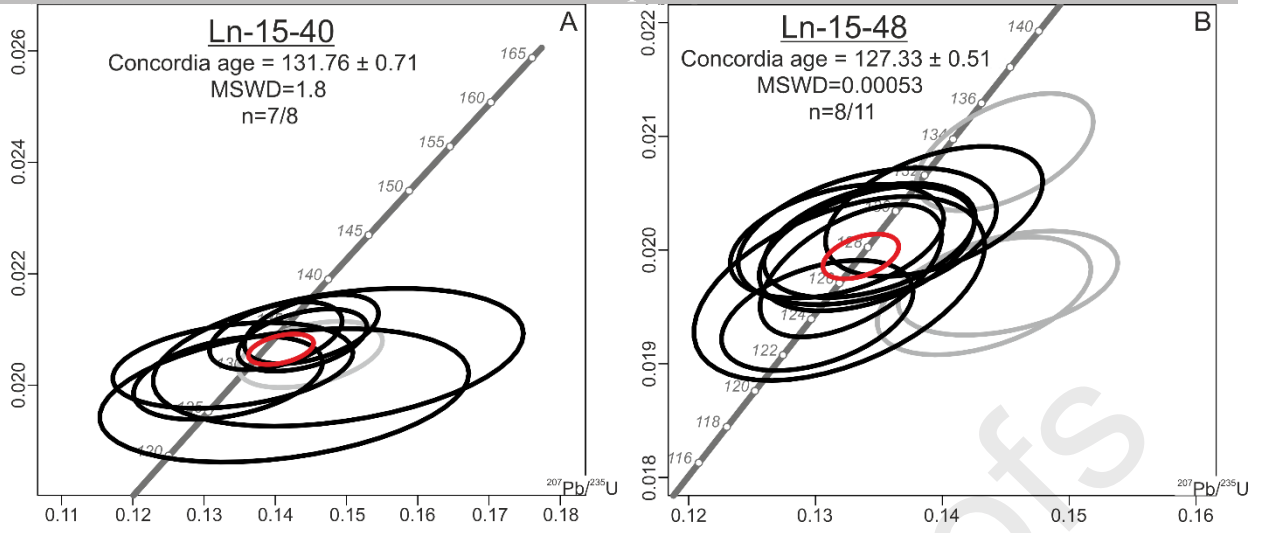
808



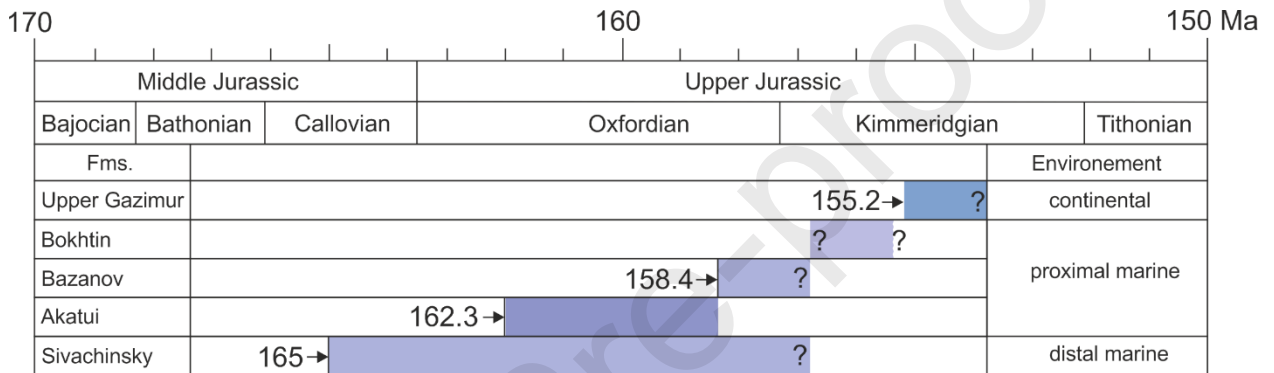
809



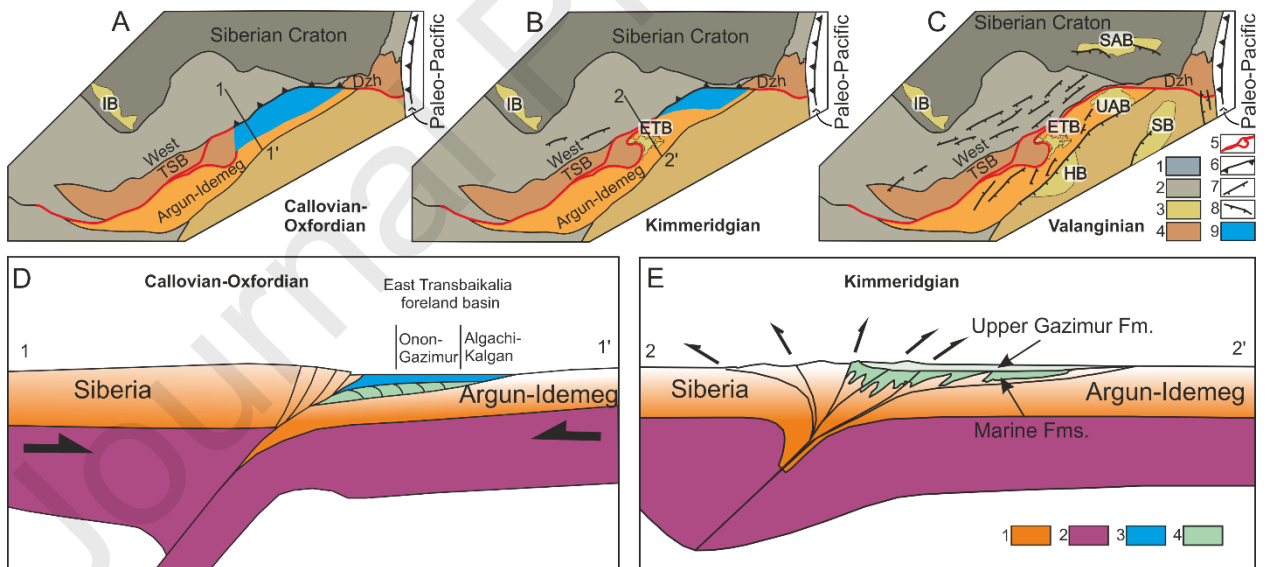




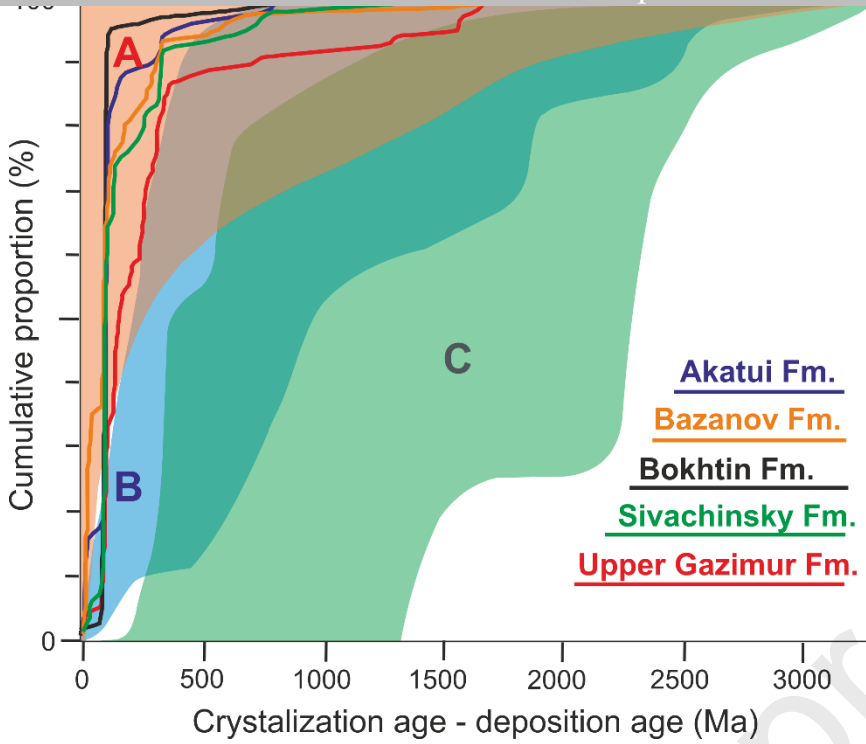
812



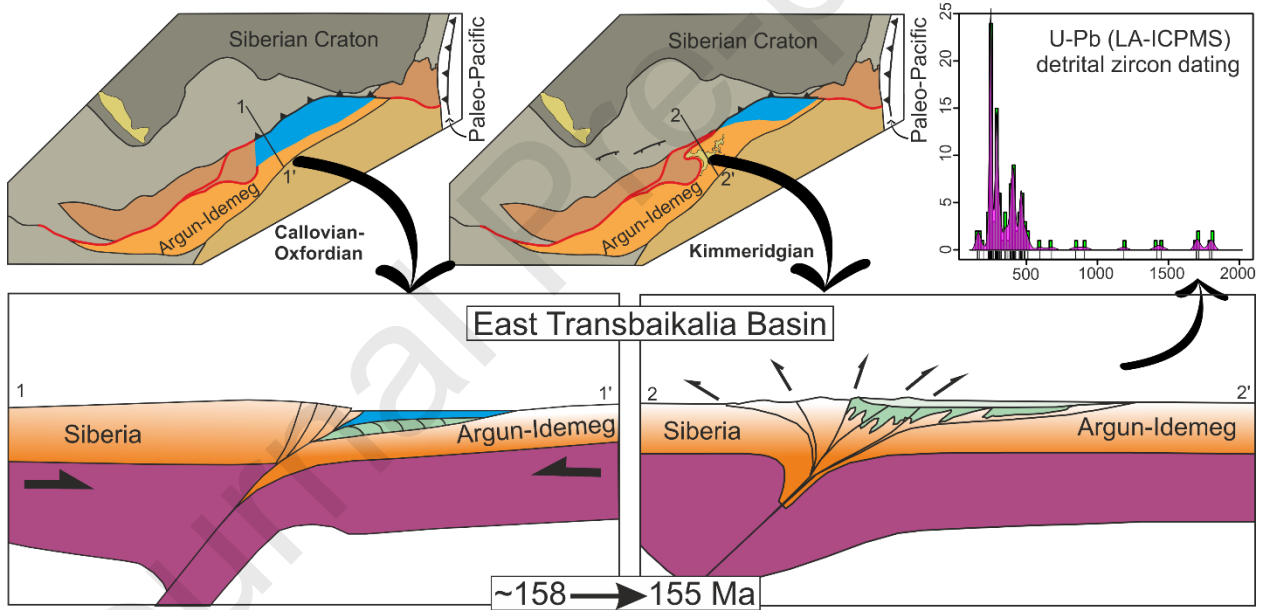
813



814



815



816